ROMA TRE
UNIVERSITÀ DEGLI STUDI

DOTTORATO DI RICERCA IN

BIOLOGIA MOLECOLARE, CELLULARE E AMBIENTALE

XXX CICLO

Role of Nerve Growth Factor (NGF) on mature and immature neurons in pathological conditions: effects of ocularly applied NGF

Ruolo del fattore di crescita neuronale (NGF) sui neuroni maturi e immaturi in condizioni patologiche: effetti del trattamento oculare con NGF

Pamela Rosso

Ph.D Candidate

Prof.ssa Sandra Moreno

Tutor

Dr.ssa Paola Tirassa

Co-tutor

Alla mia mamma e al mio papà

Alla mia gemella Ylenia
A mio marito Sergio

"Nam ut imago est animi vultus,
sic indices oculi"

"Come il volto è l'immagine dell'anima,
gli occhi ne sono gli interpreti"

Cicerone

CONTENTS

SUMMARY ..... ***V***

RIASSUNTO ..... ***IX***

SECTION I: INTRODUCTION AND OBJECTIVES

CHAPTER 1. Anatomy of the eye and visual system ***1***

CHAPTER 2. Nerve growth factor and retina-brain pathways ***8***

2.1 Nerve Growth Factor (NGF) 8

2.1.1 Mechanism of NGF retrograde signaling 12

2.2 Neurotrophins and the retina–brain pathways 14

CHAPTER 3. Ocular drug administration and effect of ed-NGF ***15***

3.1 Ocular Drug Administration and ed-NGF 15

3.2 Effects of ed-NGF in eye and brain 19

CHAPTER 4. Aim of the project ***21***

SECTION II: RESULTS

CHAPTER 5. NGF signaling in the retina of ONC model ***25***

5.1 Time-course of NGF and its receptors in ONC the retina 25

5.2 GFAP and p75NTR expression in the retina 27

5.3 Intracellular signaling in the retina 29

5.4 Effects of ONC on the structural integrity of the retina 31

CHAPTER 6. Effects of ocular application of NGF in ONC model rats....33

6.1 rhNGF intravitreal and topic delivery effects on RGC survival and axonal growth at 7 dac....33

6.2 ed-rhNGF effects on RGC survival and axon growth at 14 dac....35

6.3 Nogo-A and p75NTR immunofluorescence in optic nerves at 7 and 14 dac....37

6.4 proNGF and NGF receptor expression and activation in the retina....40

CHAPTER 7. Effects of ed-NGF in STZ-induced diabetic rats....43

CHAPTER 8. ed-NGF modulates BDNF in prefrontal cortex of diabetic rats....46

8.1 Effects of STZ and ed-NGF on body weight and behavior....48

8.2 Effect of ed-NGF on BDNF and its receptors....49

8.3 Correlation between FST latency and BDNF....52

8.4 Effects of STZ and ed-NGF on BDNF intracellular signals....54

SECTION III: DISCUSSION AND CONCLUSIONS

CHAPTER 9. Discussion and conclusions....58

9.1 Role of endogenous and exogenous NGF in the injured retina....58

9.2 Involvement of BDNF signaling in ed-NGF effects in brain....61

9.3 Conclusions....62

References....64

SUPPLEMENTARY CHAPTER - MATERIALS AND METHODS....75

SUMMARY

Nerve growth factor (NGF) was discovered by Rita Levi-Montalcini nearly 70 years ago (Levi-Montalcini et al., 1954). In the 1980s, other members of the mammalian neurotrophin family, among which brain-derived neurotrophic factor (BDNF), neurotrophin 3 (NT-3) and neurotrophin 4 (NT-4), were identified. NGF, as all neurotrophins, is synthesized as a precursor proteins (proNGF) and processed to the mature form by proteolytic cleavage (Teng et al., 2010).

During nervous system development, NGF is released by the target tissues, taken up in responsive neurons by receptor-mediated endocytosis and transported retrogradely to the cell body where it exerts biological effects through its receptors: p75NTR and TrkA (Levi-Montalcini, 1987). Complex effects of NGF are possibly related to unbalanced activation of TrkA and p75NTR. The interaction between p75NTR and proNGF has shown to induces apoptosis, and therefore to favor neurodegeneration (Cuello et al., 2010), whereas survival is mediated by NGF/TrkA interaction (Cui, 2006).
Both NGF and BDNF are involved in the regulation of central nervous system (CNS) development and extend survival, protective and regenerative action on immature and mature neurons during the entire life span (Tirassa et al., 2012). Several studies have shown that ocular tissues are also responsive to NGF. NGF also modulates retina and optic nerve development and maturation, and promotes the survival and recovery of ganglion cells, photoreceptors, and the optic nerve after experimental injuries (Carmignoto et al., 1989; Lambiase et al., 2002). The activity of NGF applied on the ocular surface as eye drops (ed-NGF) has been demonstrated in both humans and animals, and suggested as a potential treatment for ocular (Lambiase et al., 2009a) and brain degeneration (Tirassa, 2011). Indeed, through the eye surface NGF reaches the retina, and through retinal projections it acts on different brain areas, including the cortex (Calza et al., 2011; Lambiase et al., 2011).
Based on this evidences, the aim of this Ph.D project was to characterize and investigate the role of NGF in the regulation of neuronal cell survival in retina, optic nerve and brain, and to evaluate the effects of ed-NGF treatment in rat models of streptozotocin-induced (STZ) diabetes, and optic nerve crush (ONC).

The specific objectives of my Ph.D project were:
1. To investigate activated intracellular pathways and the modulation of NGF and its receptors expression in the retina and optic nerve after injury (Objective 1).

2. To verify the efficacy of ocularly applied recombinant human NGF (rhNGF) formulation to act on injured retina (Objective 2).
3. To evaluate the effects of ed-NGF treatment in diabetes-induced retinal (Objective 3), and cortical degeneration (Objective 4).

Experiments to accomplish objective 1 were carried out during the first year of my Ph.D. Unilateral optic nerve crush (ONC) was used as an experimental model of retinal injury induced by reduced retrograde support of NGF through the optic nerve. A time-course study was performed to analyze NGF signaling and the intracellular pathways involved in ONC-related injury by a combined molecular and morphological approach.

The results confirm that the nerve impairment is associated with retinal ganglion cell (RGC) loss and increase of GFAP (Glial Fibrillary Acidic Protein) and p75NTR (a member of the tumor necrosis factor (TNF) receptor superfamily) immunoreactivity in the retina within two weeks from crush. Time-course analysis of protein expression confirms the increased of GFAP and p75NGF starting from the first day after crush (dac), and also shows enhanced levels of NGF and proNGF on the second week after nerve crush.

A small but significant decrease of TrkA expression in the retinas at 14 dac was also found. Several intracellular pathways related to cell stress and death were activated in the retina early after crush (1 dac) and at all time points considered during the 14 dac.

These results support the role of proNGF/p75NTR activated cell death pathways in the retina after ONC, and suggest that crush-induced reduced availability of mature NGF is not sufficient to engage TrkA-mediated survival and neuroprotective pathways.

To support these suggestions, and evaluate the potential efficacy of ocular applied NGF to revert ONC neurodegenerative effect (Objective 2), a new set of experiments was performed during the second and third years of my Ph.D training.

The first part of the study was addressed to test two protocols of ocular NGF administration: 1) intravitreal injection with 1-1.5 µg/eye of rhNGF (ivt-rhNGF); 2) topical application of NGF on ocular surface using an eye drops NGF formulation (ed-NGF) at the concentrations of 180 and 540 µg/ml.

Morphological observations show that both ivt- and ed-NGF prevent RGC loss and stimulate axon regrowth by interfering with the apoptotic and growth inhibitory pathways at retina and nerve crush site levels, confirming that NGF reaches the retina in sufficient amounts to activate survival and protective pathways (Lambiase et al., 2005; Sposato et al., 2009). Subsequent experiments, aimed to characterize the molecular effects of ONC and ed-NGF treatment, demonstrate that NGF is able to counterbalance the ONC-induced

alteration of p75NTR/TrkA and the proNGF increase in the retina, further inducing phosphorylation of TrkA and its intracellular signals.
Evaluation of the expression of growth inhibiting factors at retina and nerve levels also indicates that ed-NGF treatment reactivates RGC-growth state and stimulates axonal regeneration.
The neuroprotective effect of ed-NGF administration was investigated and confirmed using a streptozotocin (STZ)-induced diabetes model of retinal and cortical degeneration (Objective 3). Retinopathy, one of the most common complications of diabetes mellitus, is characterized by progressive degeneration of RGCs (van Dijk et al., 2010), inflammation, leakage of blood vessels and hypoxia (Mohamed and El-Remessy, 2015). Hypervascularization in diabetes retina is associated with up-regulation of VEGF (Vascular-Endothelial Growth Factor) (Gupta et al., 2013), and altered expression of VEGF receptors on RGC, which contribute to exacerbate neurodegeneration. The set of experiments on the ed-NGF effects in STZ-retina demonstrates that ed-NGF efficiently counteracts the rise in VEGF and restores the STZ-induced reduction of VEGFR2 (vascular endothelial growth factor receptor 2) expression. Further, ed-NGF treatment blunts the *up-regulation* of proNGF and p75NTR in diabetes retina by stimulating their cleavage, and normalizes the expression of TrkA.
We also investigated a correlation between onset of depressive-like behavior and altered structure, neurotransmission, and neuronal cell death in prefrontal cortex (PFC) of diabetic rats (Objective 4).
BDNF plays a critical role in mood disorders (Dwivedi, 2013) and it is suggested as a precipitating disease marker in diabetes (Bathina and Das, 2015). However, the effects of diabetes on the BDNF and BDNF-mediated intracellular signaling in PFC were not previously described. We found that STZ induces a loss of neurons in all the layers of the cingulate (Cg1) and motor (M1) cortex. Increased expression of cleaved caspase-3 was found in the same areas, and in GAD67–positive neurons in V-VI layers. The activation of apoptotic pathways by Western Blot (WB) analysis shows enhanced caspase-3 in PFC of STZ rats. The increased levels of proBDNF and p75NTR also support the activation of cell death. In addition, the reduced phosphorylation of TrkB and AKT in STZ cortex indicates that neurotrophic survival signals are affected by diabetes. Treatment with ed-NGF normalizes the STZ-induced alterations in PFC by increasing the TrkB/p75NTR ratio and TrkB phosphorylation, and reducing the levels of proBDNF. No variation in caspase-3 was found in PFC of STZ+NGF rats when compared to controls (CTR) indicating that ed-NGF treatment does not induce an apoptotic pathway. Diabetes-induced neurodegeneration and altered BDNF signaling in PFC were

associated with onset of depressive phenotype. Indeed, compared with healthy controls, STZ rats show a significant reduction in first floating latency by forced swim test (FST), which is a widely used assay to assess antidepressant efficacy in preclinical studies (Krishnan and Nestler, 2011).
A behavioral recovery was observed following ed-NGF treatment, while no behavioral changes were found when ed-NGF was administered to healthy rats. Regression analysis shows that proBDNF and p-TrkB correlated significantly with FST data, so that when the depression phenotype is manifested, the levels of proBDNF and p-TrkB are increased and decreased respectively. These findings show, for the first time, that diabetes and its depressive phenotype manifestation are associated with altered BDNF signaling in PFC. The study also suggests that the suppression of STZ-induced depressive behavior observed in rats receiving ed-NGF might depend on NGF stimulatory action on BDNF and TrkB phosphorylation.

Overall, the results of my studies using ed-NGF as treatment in animal models of retina and brain degeneration are consistent with a growing body of evidence demonstrating that NGF might interfere with pathological processes characterized by neuronal cell loss by exerting regulatory and modulatory effects in neurons and neuronal cell precursors, glial and endothelial cells. By increasing the availability of mature NGF, ed-NGF might rebalance the Trk/p75NTR ratio to favor intracellular signals promoting survival and regrowth, stimulating neurogenesis, and plasticity. Directly or indirectly through the stimulation of other factors, NGF might be involved in the regulation of angiogenesis and inflammation. All these events could underlie NGF involvement in the control of health and disease conditions.

RIASSUNTO

Il fattore di crescita neuronale (NGF) è stato scoperto da Rita Levi-Montalcini (Levi-Montalcini et al., 1954). Negli anni Ottanta sono stati identificati nei mammiferi altri membri della famiglia delle neurotrofine, tra cui il fattore neurotrofico cerebrale (BDNF), la neurotrofina-3 (NT-3) e la neurotrofina-4 (NT-4). NGF viene sintetizzato sotto forma di proteina precursore (proNGF) e in seguito a clivaggio proteolitico trasformato nella forma matura (Teng et al., 2010).

Durante lo sviluppo del sistema nervoso, NGF viene rilasciato dai siti di sintesi, captato dai neuroni responsivi tramite endocitosi mediata dai recettori e trasportato per via retrograda al corpo cellulare dove esercita i suoi effetti biologici attraverso il legame ai propri recettori: p75NTR e TrkA (Levi-Montalcini, 1987). L'interazione tra p75NTR e proNGF induce apoptosi e di conseguenza favorisce la neurodegenerazione (Cuello et al., 2010), mentre la sopravvivenza è mediata dall'interazione tra NGF/TrkA (Cui, 2006). Sia NGF che BDNF sono coinvolti nella regolazione dello sviluppo del sistema nervoso centrale e svolgono anche un ruolo importante nella sopravvivenza, protezione e rigenerazione dei neuroni maturi o immaturi durante l'intero ciclo vitale (Tirassa et al., 2015). NGF modula anche lo sviluppo e la maturazione della retina e del nervo ottico e favorisce la sopravvivenza e la rigenerazione delle cellule gangliari, dei fotorecettori e del nervo ottico in seguito a degenerazioni (Carmignoto et al., 1989; Lambiase et al., 2002).

Di recente l'attività di NGF somministrato sulla superficie oculare come collirio (ed-NGF) è stata dimostrata sia nell'uomo che in modelli animali e suggerita come un potenziale trattamento per le degenerazioni oculari (Lambiase et al., 2009a) e cerebrali (Tirassa, 2011). NGF riesce a raggiungere la retina attraverso la superficie dell'occhio e attraverso le proiezioni retiniche agisce su diverse aree del cervello, inclusa la corteccia (Calza et al., 2011; Lambiase et al., 2011).

Scopo di questo progetto dottorale è stato caratterizzare e investigare il ruolo di NGF nella regolazione della sopravvivenza neuronale nella retina, nel nervo ottico e nel cervello, e valutare gli effetti del trattamento con ed-NGF in modelli animali di neurodegenerazione.

Obiettivi specifici del mio progetto di Ph.D sono stati:

1. Investigare l'attivazione di *pathways* intracellulari e l'espressione di NGF e dei suoi recettori nella retina e nel nervo ottico in seguito a compressione del nervo (Obiettivo 1).

2. Verificare l'efficacia del rhNGF somministrato per via oculare sulla retina danneggiata (Obiettivo 2).
3. Valutare gli effetti del trattamento con ed-NGF nella degenerazione retinica (Obiettivo 3), e corticale (Obiettivo 4) indotta dal diabete.

L'obiettivo 1 è stato portato a termine durante il primo anno di dottorato.
La lesione del nervo ottico mediante compressione unilaterale (ONC) è stata scelta come modello sperimentale di danno retinico associato al ridotto retro-trasporto di NGF attraverso il nervo ottico. Uno studio time-course è stato effettuato per analizzare la signaling di NGF e i *pathways* intracellulari coinvolti nel danno ONC-indotto secondo un approccio molecolare e morfologico. I risultati confermano che il danno del nervo è associato con la perdita delle cellule RGC e l'aumento di GFAP e p75NTR nella retina nelle due settimane successive al *crush*. L'analisi time-course conferma l'incremento della proteina fibrillare acida della glia (GFAP) e del p75NTR a partire dal primo giorno successivo al crush (dac), e mostra livelli aumentati di NGF e proNGF nella seconda settimana dopo il *crush*. È stato anche riscontrato un piccolo ma significativo decremento dell'espressione di TrkA a 14 dac. Inoltre è stata osservata l'attivazione di diversi *pathways* intracellulari correlati a stress e morte cellulare 1 dac dopo il crush e a ogni intervallo di tempo considerato durante i 14 dac.
Tali risultati illustrano il ruolo dei *pathways* di morte cellulare attivati da proNGF/p75NTR nella retina dopo ONC e suggeriscono che la ridotta disponibilità di NGF maturo non è sufficiente per innescare i *pathways* di sopravvivenza e neuroprotezione mediati da TrkA.
Per valutare dunque la potenziale efficacia di NGF applicato sulla superficie oculare nel contrastare l'effetto neurodegenerativo in seguito a ONC (Obiettivo 2), sono stati eseguiti nuovi esperimenti durante il secondo e terzo anno di dottorato. Nella prima parte dello studio sono stati testati due protocolli di somministrazione oculare di NGF: 1) iniezione intravitreale con 1-1.5 µg/eye di rhNGF (ivt-rhNGF); 2) applicazione topica di NGF sulla superficie oculare come collirio (ed-NGF) alla concentrazione di 180 e 540 µg/ml. Gli studi morfologici mostrano che entrambi i trattamenti con NGF ostacolano la perdita delle RGC e stimolano la ricrescita dell'assone interferendo con i processi apoptotici e inibitori della crescita a livello della retina e del sito di crush del nervo. Questo conferma che NGF raggiunge la retina in quantità sufficienti ad attivare i *pathways* di sopravvivenza e protezione (Lambiase et al., 2005, Sposato et al., 2009).
Successivi esperimenti indirizzati a caratterizzare gli effetti molecolari di ONC e di ed-NGF dimostrano che NGF è in grado di controbilanciare l'aumento di p75NTR/TrkA indotto da ONC e l'aumento di proNGF nella retina, inducendo

ulteriormente la fosforilazione di TrkA e dei suoi segnali intracellulari. La valutazione dell'espressione dei fattori di inibizione della crescita a livello della retina e del nervo ha anche indicato che il trattamento con ed-NGF riattiva lo stato di crescita delle RGC e stimola la rigenerazione assonica.
L'effetto neuroprotettivo della somministrazione con ed-NGF è stato studiato e confermato utilizzando il modello di diabete indotto da streptozotocina (STZ) che induce degenerazione retinica e corticale (Obiettivo 3). La retinopatia, tra le più comuni complicazioni del diabete mellito, è caratterizzata dalla progressiva degenerazione delle cellule RGC (van Dijk et al., 2010),), da infiammazione, perdita dei vasi sanguigni e ipossia (Mohamed and El-Remessy, 2015). L'ipervascolarizzazione nella retinopatia diabetica è associata all'aumento della regolazione del fattore di crescita dell'endotelio vascolare (VEGF) (Gupta et al., 2013) e all'alterata espressione dei recettori VEGF sulle RGC, la quale contribuisce ad aggravare la neurodegenerazione. Gli esperimenti sugli effetti di ed-NGF nella retina STZ hanno dimostrato che ed-NGF contrasta efficacemente l'aumento del VEGF e ripristina la riduzione dell'espressione di VEGFR2 indotta da STZ. Inoltre, il trattamento con ed-NGF contrasta l'up-regulation di proNGF e di p75NTR nella retina, stimolandone il clivaggio e normalizzando l'espressione di TrkA.
Abbiamo anche analizzato la correlazione tra l'insorgenza di un fenotipo comportamentale indicato come depresso (depressive like phenotype), le alterazioni morfologiche e biochimiche, la neurotrasmissione e la morte neuronale nella corteccia prefrontale (PFC) (Obiettivo 4).
Il BDNF svolge, infatti, un ruolo fondamentale nei disturbi dell'umore (Dwivedi, 2013) ed è suggerito come un marker di aggravamento nel diabete (Bathina and Das, 2015), ma gli effetti del diabete sul signaling intracellulare di BDNF nella PFC non sono stati precedentemente studiati. I risultati del mio studio dimostrano che STZ induce una perdita di neuroni in tutti gli strati della corteccia cingolata (Cg1) e motoria (M1). Una maggiore espressione della caspasi-3 è stata riscontrata nelle stesse aree, mentre i neuroni GAD67-positivi sono stati osservati negli strati V-VI. L'attivazione di *pathways* apoptotici mostra un incremento della caspasi-3 nella PFC dei ratti diabetici. L'incremento dei livelli di proBDNF e p75NTR supporta l'attivazione dei processi di morte cellulare. Inoltre, la ridotta fosforilazione di TrkB e AKT nella corteccia dei ratti diabetici indica che i segnali neurotrofici di sopravvivenza sono influenzati dal diabete.
Il trattamento con ed-NGF normalizza le alterazioni indotte da STZ nella corteccia prefrontale mediante l'incremento del rapporto tra TrkB/p75NTR e la fosforilazione di TrkB, e la riduzione dei livelli di proBDNF. Nessuna variazione dei livelli della caspasi-3 è stata trovata nella PFC dei ratti

STZ+NGF quando comparati con i controlli (CTR), indicando che il trattamento con ed-NGF non induce il processo apoptotico.
La neurodegenerazione indotta dal diabete e l'alterato signaling di BDNF nella PFC sono associati con l'insorgenza del fenotipo depressivo. Infatti, rispetto ai controlli sani i ratti diabetici mostrano una significante riduzione della latenza nel forced swim test (FST), un test ampiamente utilizzato per valutare l'efficacia antidepressiva negli studi preclinici (Krishnan and Nestler, 2011). Un recupero comportamentale è stato osservato nei ratti STZ trattati con ed-NGF, mentre nessun cambiamento comportamentale è stato trovato con ed-NGF somministrato in ratti sani. L'analisi di regressione mostra che proBDNF e p-TrkB sono correlati in modo significativo ai dati FST: quando si manifesta il fenotipo depressivo i livelli di proBDNF e p-TrkB aumentano e diminuiscono rispettivamente. Questi risultati dimostrano, per la prima volta, che il diabete e la manifestazione del fenotipo depressivo sono associati a un'alterazione della signaling di BDNF nella PFC. Lo studio suggerisce inoltre che l'inibizione del comportamento depressivo indotto da STZ osservata nei ratti che ricevono ed-NGF potrebbe dipendere dall'azione stimolante di NGF sul BDNF e sulla fosforilazione di TrkB.

Nell'insieme, i risultati dei miei studi che utilizzano ed-NGF come trattamento nei modelli animali di degenerazione retinica e cerebrale concordano con altri studi nel dimostrare la possibile interferenza di NGF nei processi patologici che coinvolgono una perdita di cellule neuronali. NGF esercita effetti regolatori e modulatori in diversi tipi cellulari, tra cui i neuroni e i precursori delle cellule neuronali, le cellule gliali e le cellule endoteliali.
Aumentando la disponibilità di NGF maturo, ed-NGF potrebbe riequilibrare il rapporto Trk/p75NTR per favorire i segnali intracellulari che promuovono la sopravvivenza e la ricrescita, stimolando la neurogenesi e la plasticità. Direttamente o indirettamente, attraverso la stimolazione di altri fattori, NGF potrebbe essere coinvolto nella regolazione dell'angiogenesi e dell'infiammazione. Tutti questi eventi potrebbero essere alla base del coinvolgimento di NGF nel controllo delle condizioni di salute e malattia.

Section I

INTRODUCTION AND OBJECTIVES

CHAPTER 1
ANATOMY OF THE EYE AND VISUAL SYSTEM

The eye is anatomically a fused two-piece unit composed of the anterior and posterior segments filled with fluids named aqueous and vitreous humor, which nourish the internal structures and generate a pressure to maintain eyeball shape (Lambiase et al., 2011; Patel et al., 2013). The anterior ocular segment comprises cornea, conjunctiva, iris, ciliary body, and lens, while the posterior ocular segment extends from the back surface of the lens to the retina and includes sclera, choroid, retinal pigment epithelium, neural retina and optic nerve (Fig 1.1).

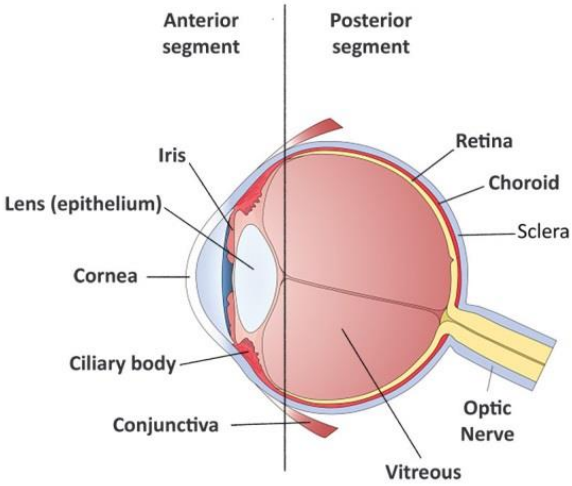

Fig. 1.1 Anatomy of the eye.
The vertical line divides the structures belonging to the anterior segment (cornea, iris, lens and ciliary body) from those the posterior segment, including the conjunctiva, sclera, choroid and retina (*Modified from Tirassa et al., 2017*).

Although the retina and part of the optic nerve are localized outside the cranial cavity, they are part of the central nervous system (CNS), since during embryogenesis they originate from evaginations of the lateral portions of the anterior neural tube that form the optic vesicles (Lamba et al., 2008). The retina is the structure that transforms light into nerve signals and discriminates wavelengths into a selected range (visible spectrum). It is formed by different layers of interconnected nerve cell bodies organized in nuclear and synaptic layers. The outer nuclear layer (ONL) contains two types of photoreceptors (rods and cones), one of the most specialized and complex cells in the nervous system. Rods are more numerous than cones and are sensitive to half-light vision but not bright light, while cones do not respond to half-light but require much brighter light. The photoreceptors convert light energy into electrical signals through a process known as phototransduction. Retinal interneurons further codify the electrical signals into optic nerve impulses, which are interpreted by the brain (Cuenca et al., 2014).

Adjacent to the photoreceptor layer is the retinal pigmented epithelium (RPE) which is essential for the maintenance of rods and cones, and is a source of retinal pluripotent cells which can generate new photoreceptors, glia cells, and neurons (Ahmad et al., 2000; Tropepe et al., 2000; Lamba et al., 2008).

The inner nuclear layer (INL), comprises different retinal cell classes of interneurons: 1) bipolar cells transfer the visual information from photoreceptors to retinal ganglion cells (RGCs); 2) amacrine cells that are inhibitory interneurons between bipolar cells and RGCs; 3) horizontal cells that regulate the activity of photoreceptors and transfer the information to bipolar cells by connections parallel to the retinal layers (Garcia et al., 2017). Bipolar cells occupy a strategic position in the retina since all signals originating from photoreceptors propagated to the ganglion cells must pass through them (Luo et al., 2008). The ganglion cell layer (GCL) contains the cell bodies of RGCs whose axons form the nerve fiber layers that converge in the optic disc to form the optic nerve. At the outer plexiform layer (OPL) the dendrites of horizontal and bipolar cells make synaptic contacts with the axonal termination of the photoreceptors (Cuenca et al., 2014). The synaptic contacts between RGCs, bipolar and amacrine cells are localized in the inner plexiform layer (IPL) (Fig. 1.2) (Garcia et al., 2017).

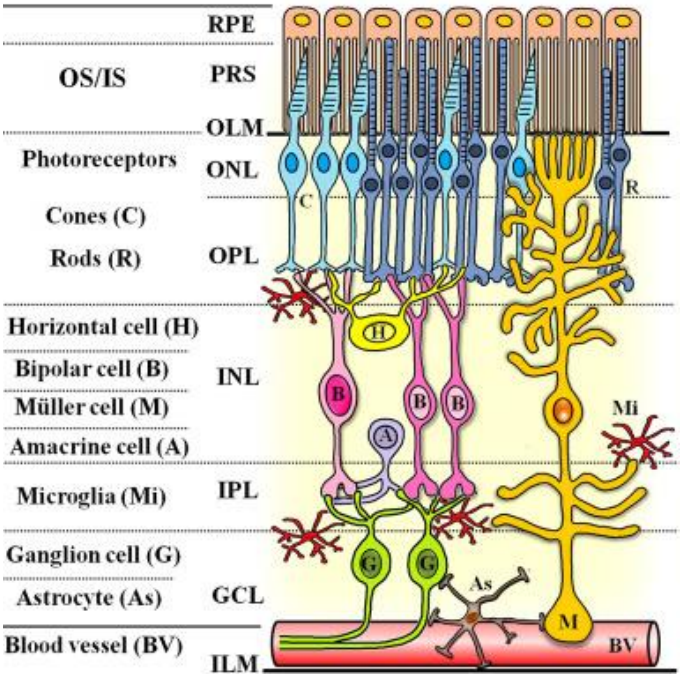

Fig. 1.2 The retina layers. The figure shows an enlarged scheme of the retinal layers and cell type distribution. The photoreceptors are at the top of this picture, close to the retinal pigment epithelium. The bodies of horizontal (H) and bipolar cells (B) compose the inner nuclear layer. Amacrine cells (A) lie close to ganglion cells (G) near the surface of the retina. Axon-to-dendrite neural connections make up the plexiform layers separating rows of cell bodies (Modified from Garcia et al., 2017).

Apart from neurons and photoreceptors, other representative retinal cells are the Müller cells, microglial cells, and astrocytes, that passes through all retinal layers and are responsible for homeostatic and metabolic support of the retina. Müller cells are located in the INL, whereas their processes expand

throughout the neural retina. Astrocytes are restricted to the nerve fiber/ganglion cell layers (Garcia et al., 2017). Indeed, in the healthy retina Müller cells regulate not only glucose metabolism, water homeostasis and pH, but also neuronal cell signaling processes and neurotransmitter uptake (Newman, 2015). Similar to astrocytes, Müller cells become activated after injury with up-regulation of intermediate filament proteins such as glial fibrillary acidic protein (GFAP) and vimentin (Cuenca et al., 2014). Activated astrocytes and Müller cells constitute a process called reactive gliosis, which has an acute neuroprotective effect but, as it persist chronically after injury, it limits regeneration and exacerbates neurodegeneration, causing direct and indirect damage to neurons. It is important to mention also the fovea, a central region of the retina containing a very high concentration of cones responsible for a great visual acuity and color estimation (Cuenca et al., 2014).

The eye and brain areas receiving retinal inputs constitute the visual system. In all mammals, including humans, vision is guaranteed by the integrity of retinofugal pathways that transfer information from the eye to the brain visual areas, and by the survival and regulatory inputs retrogradely directed to the retina (Kaas and Balaram, 2014). The electrical information is transmitted to the ganglion cells, which send out impulses through their axonal prolongations connecting the retina to the brain via the optic nerves that meets at the optic chiasm. This is the point where images from the right visual field are transmitted to the left half of the brain (green part of the Fig. 1.3), whereas images from the left visual field are projected to the right hemisphere (red part on the Fig. 1.3). One half of the information from each eye (from the nasal part of the retina) crosses sides, whereas the other half (temporal part) stays on the same side. The main visual pathway is the retina-geniculate-striate pathway, which begins with RGC axonal projections to the lateral geniculate nucleus of the thalamus (LGN). The LGN receives information from the retina and sends projection to the primary visual cortex (V1, Brodmann area 17, striate cortex) via the optic tract. A part of the projection from the eyes is transferred to the superior colliculus (SC), a part of optic tectum in the vertebrate midbrain which is involved in saccadic (fast) eye movements and eye-hand coordination. Finally, electrical signals from the RGCs reach the primary visual cortex (Yantis, 2014), where they are further processed and analyzed and can be sent to higher order visual areas**.** The retina topographic organization is preserved in the set of connections to

the LGN and cortex (Kaas and Balaram, 2014), to guarantee correct spatial orientation of visual information (Fig. 1.3).

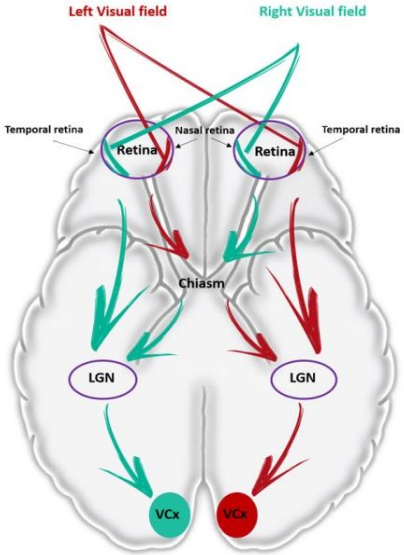

Fig. 1.3 Primary visual pathway. RGC axons exit the eyes *via* the optic nerve, partially cross at the optic chiasm, and form two optic tracts, which combine inputs from the ipsilateral temporal hemiretina and the contralateral nasal hemiretina. Visual information is transmitted by RGC axons to the LGN and visual cortex where the topographic representation of the retina visual map is preserved (*Modified from Tirassa et al., 2017*).

A second pathway, the extrastriate pathway, plays a role in visual perception and attention, and is thought to mediate action blind sight (Bear et al., 2007; Erskine and Herrera, 2014; Kaas and Balaram, 2014). A third retinohypothalamic pathway that contributes to regulating the circadian system has also been identified (Berson et al., 2002; Hattar et al., 2002). It is principally associated with a restricted RGC type, the intrinsically photosensitive ganglion cells (ipRGCs) localized in the inner retina layer. Retrograde tracing experiments in animal models and neuroimaging analysis in humans confirm that ipRGCs project directly to the suprachiasmatic nucleus (SCN) through the retinohypothalamic tract (RTH), but also show a widespread brain projection pattern from and to the SCN. Direct projections

of ipRGCs to the amygdala have been described in rodents and a retina-amygdala functional pathway, passing through the superior colliculi and the thalamus, has also been found in humans (Elliott et al., 1995). In addition, the hippocampus, the paraventricular and supraoptic nuclei (other hypothalamic nuclei) are secondarily influenced by the non-image-forming system through the locus coeruleus, which also receives projections from the SCN (Elliott et al., 1995; Aston-Jones et al., 2001).

Light inputs to SCN also involve the dopaminergic mesocorticolimbic pathway, called the reward circuit, whose core is the ventral tegmental area that projects to the nucleus accumbens; information then flows to the subcortical limbic areas like amygdala, hippocampus and hypothalamus, and finally to the prefrontal cortex and anterior cingulate cortex (Borsook et al., 2007). The diurnal variation of dopaminergic transmission in the mesocorticolimbic structures is dependent on the SCN and clock gene expression, thus supporting a functional correlation between the anatomical substrates for cognition/emotion, reward and light stimuli (Sleipness et al., 2007; Hampp et al., 2008). An integrated view of the anatomical network for visual and reward signals is illustrated in Fig. 1.4 (Tirassa et al., 2017, *In press*).

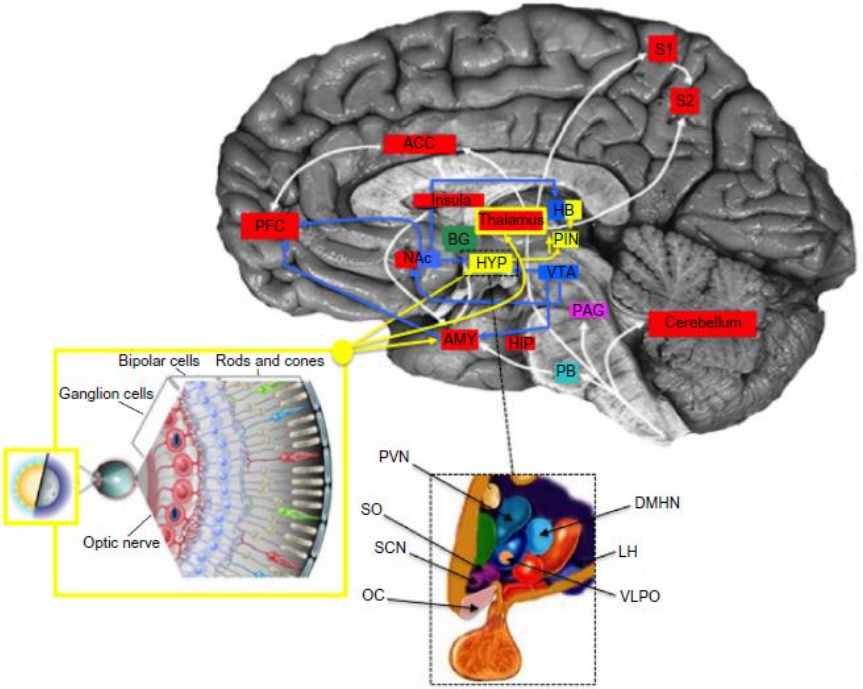

Fig. 1.4 Anatomical brain structure and pathways involved in visual and reward signals. The suprachiasmatic nucleus (SCN), the pineal (PIN) and the habenular nucleus (HB) receive direct projections RGCs, although their activities are also modulated by the reward system via the ventral tegmental area (VTA) and nucleus accumbens (NAc). The circadian rhythm and functions of the hypothalamic nuclei are regulated by light signals through the SCN and by the reward system by the VTA/NAc network.
Abbreviation: Anterior cingulate cortex (ACC); dorsomedial hypothalamic nuclei (DMHN); lateral hypothalamus (LH); hippocampus (HIP); optic chiasm (OC); parabrachial nucleus (PBN); periaqueductal grey (PAG); somatosensory cortex (S1; S2); supraoptic nucleus (SO); ventrolateral preoptic nucleus (VLPO) (*Tirassa, et al., 2015, with permission from Dove Medical Press Ltd).*

CHAPTER 2
NERVE GROWTH FACTOR AND RETINA-BRAIN PATHWAYS

2.1 Nerve Growth Factor (NGF)

Four neurotrophins have been identified in mammals: nerve growth factor (NGF), brain-derived neurotrophin factor (BDNF), neurotrophin 3 (NT3) and neurotrophin 4 (NT4; also known as NT5). Nerve growth factor (NGF), the first neurotrophin factor to be characterized, was discovered during a search for survival factors (Levi-Montalcini, 1987; Reichardt, 2006).

Besides playing a critical role in the growth and survival of peripheral sensory and sympathetic neurons (Levi-Montalcini and Angeletti, 1968; Miller and Kaplan, 2001), NGF is also important for the maintenance and regeneration of specific neuronal populations in the adult brain. Neurotrophins are synthesized in the endoplasmic reticulum as pre-proproteins, and cleavage of the signal peptide of pre-proproteins converts these into pro-neurotrophins. In the trans-Golgi network and in secretory vesicles, pro-neurotrophins dimerize and are proteolytically processed by enzymes to their mature forms before their release from the cell (Longo and Massa, 2013).

Experimental evidence demonstrated that pro-neurotrophins, as well as mature neurotrophins, exert biological activity. Notably, pro- and mature neurotrophin functions are mediated by two distinct receptors: Trk and p75NTR.

The first neurotrophin receptor to be discovered was p75NTR (Chao, 1994) that was identified as a low-affinity receptor for NGF, but subsequently was shown to bind all neurotrophins and also pro-neurotrophins (Lee et al., 2001). In contrast, a second group of neurotrophin receptors are members of the

tropomyosin-related kinase (Trk) family and are more selective for neurotrophin ligand binding.

Trk receptors: there are three type of Trk receptors that bind to different neurotrophins: NGF binds to TrkA; Brain-derived neurotrophic factor (BDNF) and Neurotrophin-4 (NT4) bind TrkB and Neurotrophin-3 (NT3) binds to TrkC.

TrkA is a tyrosine kinase receptor with a molecular weight of 140 kDa (Kaplan et al., 1991). Its extracellular domain is connected to the intracellular domain by a single transmembrane segment, and consist of a cysteine-rich cluster followed by three leucine-rich repeats, another cysteine-rich cluster and two immunoglobulin-like domains (Reichardt, 2006). The immunoglobulin-like domains, proximal to the membrane, are sufficient for assuring NGF binding. The intracellular domain contains a tyrosine kinase domain and several tyrosine residues that are phosphorylated upon receptor activation (Wiesmann and de Vos, 2001).

TrkA leads to neuronal cell survival through the activation of three main tyrosine kinase-mediated pathways. PI3K-AKT axis (phosphatidylinositol-3 kinase/Ak Trasforming) is the most well studied NGF survival pathway. The activation of PI3K through Ras or Gab1 promotes survival and growth of neurons and other cells. The induction of MAPK-ERK (mitogen-activated protein kinase/extracellular signal-regulated kinase) pathway is responsible for TrkA-induced neuronal cell differentiation. In addition, phospholipase Cγ1 (PLCγ1)-PKC pathway mediates synaptic plasticity (Cui, 2006; Reichardt, 2006; Longo and Massa, 2013). Overall, the effects induced through these signaling pathways promote cell survival and differentiation (Fig. 2.1) (Huang and Reichardt, 2003).

p75NTR receptor: p75NTR is a member of the tumor necrosis factor (TNF) receptor superfamily. P75NTR has four cysteine-rich repeats that are all required for ligand binding (He and Garcia, 2004). Its extracellular domain (p75ECD) is connected to its intracellular domain (p75ICD) by a single transmembrane region. The intracellular domain contains several sites that function as a binding region for adaptor proteins (Roux and Barker, 2002). p75NTR also contains cleavage sites for γ-secretase in its intracellular domain and α-secretase in its extracellular domain.

Similarly to TrkA, p75NTR regulates different signaling pathways. For instance, this receptor induces a signaling cascade converging on NF-κB (nuclear factor-κB) activation, which results in the transcription of several

multiple genes, including promoters of neuronal cell survival. The activation of JNK (c-jun N-terminal kinase) pathway also controls the activation of a plethora of genes, some of which are involved in neuronal cell apoptosis. p75NTR also regulates the activity of RhoA, which controls growth cone mobility and cytoskeleton remodeling. The p75NTR-induced effects are diverse and include cell survival, cell death, regulation of proliferation and inhibition of neurite outgrowth, depending of the expression of the Trk receptors, sortilin and diverse intracellular signaling adaptors (Fig. 2.1) (Longo and Massa, 2013).

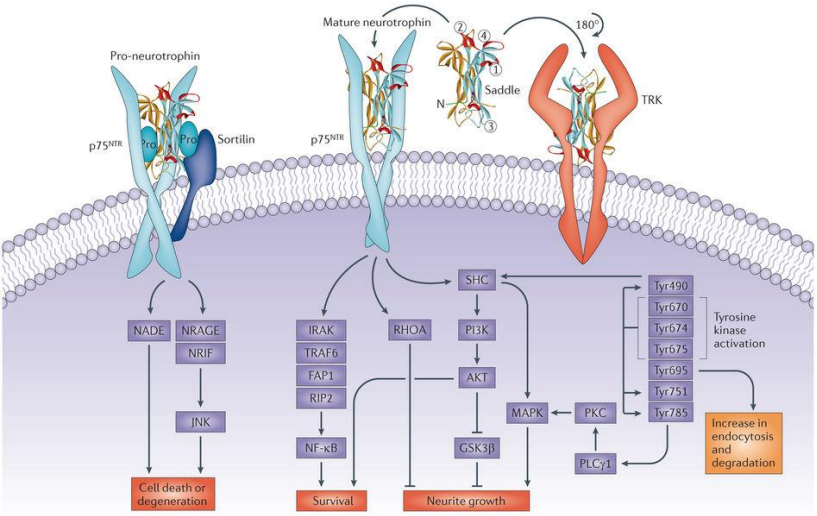

Fig. 2.1 Neurotrophin signaling pathways. TRK ligand binding by mature neurotrophins results in the phosphorylation of an array of intracellular domain tyrosine residues, which activate kinase activity resulting in further receptor autophosphorylation. This phosphorylation forms adaptor binding sites that couple the receptor to MAPKs, phosphoinositide 3‑kinase (PI3K) and phospholipase Cγ1 (PLCγ1) pathways, and may promote neurite outgrowth, differentiation and cell survival. Mature neurotrophins binding to p75NTR, may augment neurotrophin binding to TRK receptors, reinforce TRK signaling through AKT and MAPKs, and further promote survival through NF‑κB pathway, or antagonize the actions of TRK through the activation of JNK and RHOA pathways. Pro-neurotrophin binding in complex with sortilin selectively activates cell-death-related pathways (Longo and Massa, 2013).

Accumulating evidence suggests that NGF-dependent effects are mediated not only by the binding to TrkA/TrkA or p75NTR/p75NTR homodimers, but also by the formation of molecular complexes with diverse co-receptors, which confers specificity to neurotrophin signaling. Indeed, mature NGF can bind to a complex of p75NTR and TrkA. In this context, p75NTR association to TrkA increases NGF binding and enhances NGF-mediated TrkA activation, inducing pro-survival actions (Fig. 2.2). On the contrary, proNGF preferentially binds to a complex of p75NTR and Sortilin, another type I transmembrane protein, but structurally unrelated to p75NTR. This latter event is able to promotes the activation of pro-apoptotic pathways which lead to neuronal cell death (Almeida and Duarte, 2014) (Fig. 2.1 and Fig. 2.2). Thus, it is clear that changes in the ratio of Trk/p75NTR and pro-NGF/NGF can dramatically contribute to dysbalances in the activation of survival/apoptotic pathways in neuronal cells occurring during pathological conditions.

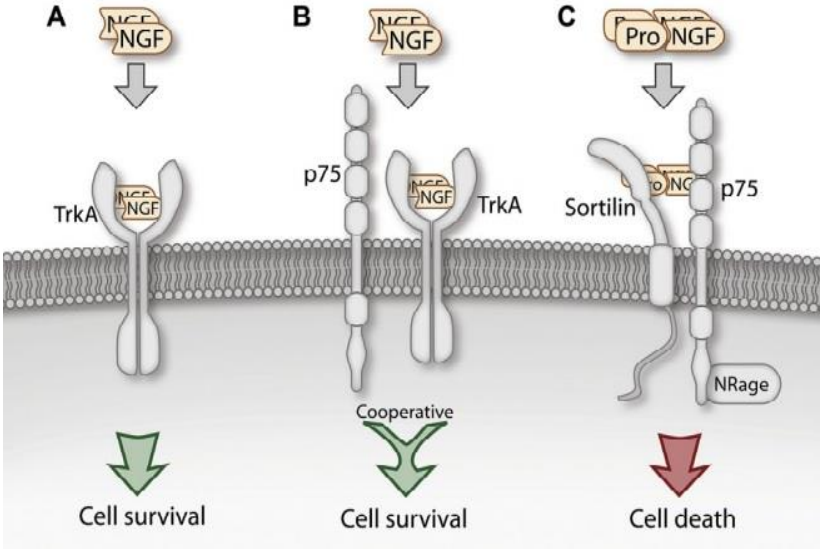

Fig. 2.2 Effects of NGF and its receptors on cell death and survival. (A) The neurotrophin NGF binds to TrkA to promote the survival of central neurons. (B) when both receptors are coexpressed TrkA-mediated survival after NGF binding is enhanced. (C) pro-NGF can initiate cell apoptosis by binding to a p75NTR-sortilin complex (Almasieh et al., 2012).

2.1.1 Mechanism of NGF retrograde signaling

NGF biological actions, such as survival and differentiation, are performed through retrograde axonal transport by which NGF captured by the nerve endings reaches the cellular body moving along the axon. Through this retrograde transport, NGF reaches target cell soma where it triggers several metabolic events (Maday et al., 2014).

Neurotrophic effects require internalization of the ligand–receptor complex, and its retrograde transport toward the cell body. The internalization of NGF occurs through a clathrin-dependent mechanism that requires TrkA and Dynamin (Zhang et al., 2000; Roux and Barker, 2002; Cosker et al., 2008). The kinase activity of TrkA appears crucial for this process (Reynolds et al., 1998) since inhibition of TrkA-mediated PI3K activity blocks retrograde transport of NGF in sensory and sympathetic neurons (Reynolds et al., 1998; Reynolds et al., 1999; Roux and Barker, 2002).

p75NTR has also been implicated in the axonal transport of neurotrophic factors and the receptor has been shown to be transported both anterogradely and retrogradely in the sciatic nerve (Johnson et al., 1987). In the absence of TrkA, p75NTR is capable of internalizing NGF (Kahle et al., 1994), and transporting NGF retrogradely from the retina to the isthmo-optic nucleus (Von Bartheld et al., 1996).

These retrograde signals of NTs are highly relevant to the identification of treatments for major neurodegenerative diseases (Fig. 2.3).

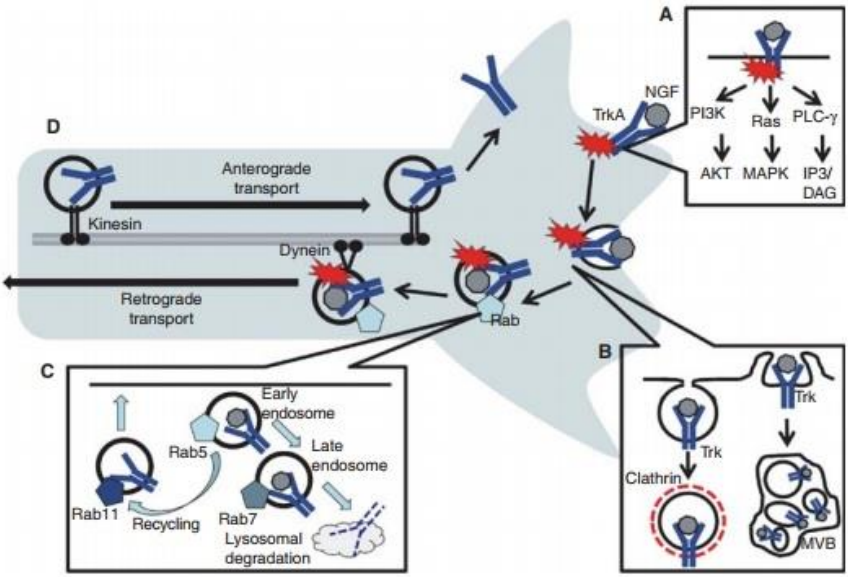

Fig. 2.3 Retrograde and anterograde signaling of NGF. (A) Trk receptors are activated and recruit PI3 kinase, Ras/MAPK, and PLC-γ to initiate downstream signaling pathways. (B) Internalization of neurotrophin/Trk complexes can occur via clathrin-dependent mechanisms to give rise to early endosomes, or via macropinocytosis, which gives rise to multivesicular bodies (MVBs). (C) The endosomal pathway involves maturation from early endosomes associated with Rab5 to late endosomes associated with Rab7. Vesicles are degraded in lysosomes or can be recycled back to the membrane through association with Rab11. (D) In neurons, endosomes are transported along the axon by dynein-mediated retrograde transport toward the cell body, or by kinesin-mediated anterograde transport toward the distal axon (Cosker and Segal, 2016).

2.2 Neurotrophins and the retina–brain pathways

Investigations on the role of neurotrophins in the regulation of visual system development and functional acquisition started in the 1980s, when NGF, BDNF and their receptors were found in the retina, optic nerve, and brain visual areas, and retrograde transport of NGF through the optic nerve was demonstrated (von Bartheld, 1998).

In the retina, NGF is produced and utilized by RGCs, bipolar neurons and glial cells, in a local paracrine/autocrine fashion (Balzamino et al., 2015). Experimental data indicate that both exogenous and endogenous neurotrophins can be anterogradely transported through the optic nerve (Carmignoto et al., 1991; Wahle et al., 2003). In RGCs, neurotrophins are not rapidly degraded after internalization, but are differently sorted by a mechanism regulated by Trk receptors, so that NGF is mainly targeted to lysosomes, while BDNF is recycled to the surface membrane. Neurotrophin receptors are also rapidly recycled, implying a regulation of receptor density on axons and dendrites which has important consequences for their coupling to distinct neurotrophin ligands (Zhang et al., 2000; Butowt and von Bartheld, 2001).

Thus, the network between eye and brain, together with the anterograde and retrograde transport of neurotrophins through the optic nerve represent an integrated system by which the retinal response is centrally regulated and, conversely, retinal input modulates central activities and functions. Besides innervating, primary visual areas, RGCs extend direct projections to the RTH tract. In addition, RGCs directly and indirectly project to limbic structures, including the hippocampus and septum (Teng et al., 2005; Hatori and Panda, 2010). Through these networks, light and visual stimuli can regulate physiological functions, including arousal and cognition (Vandewalle et al., 2007; Vandewalle et al., 2009). In this context, the central cholinergic system, which is the brain's principal NGF and BDNF target, is also a fundamental element in the regulation of visual cortex plasticity (Picciotto et al., 2012). It contributes to integrate emotional and cognitive components of visual information by acting on the hippocampus and frontal cortex (LeGates et al., 2014). Furthermore, the cholinergic forebrain neurons also modulate the activity of the SCN, guaranteeing the circadian rhythmicity receiving direct input from the retina (Hut and Van der Zee, 2011).

CHAPTER 3

OCULAR DRUG ADMINISTRATION AND EFFECT OF ed-NGF

3.1 Ocular Drug Administration and ed-NGF

Topical drops, together with intravitreal, subconjunctival, and retrobulbar injection, represent the most common routes of ocular drug administration. These methods - which show differences in the bio-distribution of drugs in dependence of their dimension and physico-chemical characteristics - can be used alone or in combination to treat different ocular diseases affecting the anterior and/or posterior segments of the eye. The eye presents anatomical and physiological barriers which limit the absorption and/or transport of molecules thought its tissue layers. These factors affect the efficacy of drugs on the ocular surface, or their accessibility to the posterior segments (Fig. 3.1 A).

In general, intravitreal injection and topical application are at opposite ends in terms of bioavailability and efficacy on the retina, being conceived, respectively, for direct drug delivery to the posterior segment and treatment of the anterior segment (Patel et al., 2013) (Fig. 3.1 B).

A

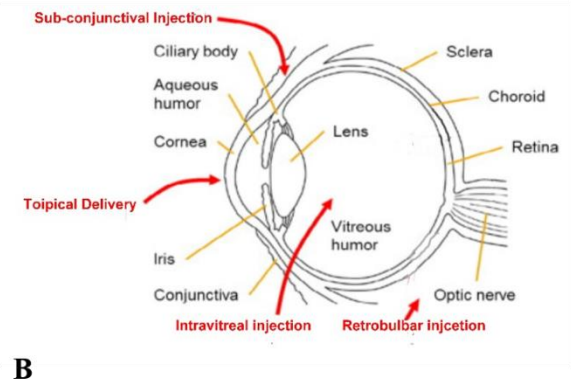

B

	Intravitreal Injection	**Topical drops**
Pathway to target posterior segment	Direct	Mainly no-trans-corneal ways
Anatomical barriers	Vitreous, Retina	Conjunctiva, Sclera, Choroid, RPE, Retina
Risk Adverse effects	High injection risk Vitreous hemorrhage, retinal detachment	Safety, moderate systemic effect Conjunctival irritation
Peak bioavability Intravitreal Intra-aqueous humor	 100% 3%	 0,0004% 0,0007-5%
Distribution	Local	Local and systemic washout
Duration of action	1-7 days	½-6 hours

Fig. 3.1 Drug delivery to the eye. (A) Intraocular, periocular injection and topical application. Diffusion and efficacy of a drug's action on the posterior segment of the eye depends on its physical and biological characteristics, and by the static and dynamic ocular barriers. (B) The table shows the differences between intravitreal and eye drop (*Modified from Tirassa et al., 2017*).

However, following topical application, also as eye drops, drugs are capable of reaching the back of the eye, although in low concentration (Maurice, 2002; Hughes et al., 2005). The trans-corneal and trans-conjunctive/sclera pathways are the most suitable route for topically applied drugs to reach the retina. Specifically, drugs can penetrate into the posterior segments by three main routes: 1) diffusion through the conjunctiva, sclera, and choroid; 2) clearance into the systemic circulation and secondary re-entering of the eye; 3) lateral diffusion from the conjunctiva into iris/ciliary body, and thus into the anterior chamber and other intraocular tissues (Fig. 3.2). Despite extremely low bioavailability of topical delivery, this route of ocular drug administration is quite appealing, as it reduces the chance of systemic side-effects and is minimally invasive. In addition, topical approaches to retinal disease can be convenient, self-administered, and can lower the overall treatment burden for chronic diseases.

Intraocular and eye drop administration of NGF both exert biological effects on the posterior segment of the eye in different animal species, such as mouse (Lambiase and Aloe, 1996), rat (Tirassa et al., 2015) and rabbit (Lambiase et al., 2002). In humans, ed-NGF is safe (Falsini et al., 2016), improves visual acuity and electro-functional retina activity (Lambiase et al., 2009a), and induces prolonged neuroprotective effects which result in stabilization/improvement of visual function even after short treatment times (Falsini et al., 2016). These data highlight the ability of ed-NGF to reach the posterior segments and exert an action on neuronal cells, even though the molecular weight of its bioactive form (about 14.5 kDa) would not predict passage through the cornea. A study using radiolabeled NGF demonstrated the presence of NGF in the conjunctiva, sclera, choroid, retina, and optic nerve, but not in corneal stroma. The maximum absorption was at 6 hours after ed-NGF, although [I^{125}]NGF was detected already at 2 hours in the optic nerve and, to a lesser extent, in the retina. The radiolabeled signal disappeared in all ocular tissues at 48 hours after ed-NGF administration (Lambiase et al., 2005). These observations were confirmed by analyzing the pharmacokinetics and dose-response of ed-NGF. A single administration of ed-NGF was sufficient to increase NGF content in the retina, optic nerve, and sclera but not in lens. Compared to basal values, NGF increases were found also in all tissues of the untreated contralateral eye.

Based on the ocular penetration route for topically applied drugs illustrated in Fig. 3.2, it is likely that ed-NGF reaches the posterior segment of the eye by trans-conjunctive/trans-sclera pathways. Moreover, the rapid and marked

uptake of radiolabeled NGF by the optic nerve may also result from passage through the retrobulbar space as well as systemic absorption. The effects on the contralateral eye and the NGF peak in serum might support this hypothesis.

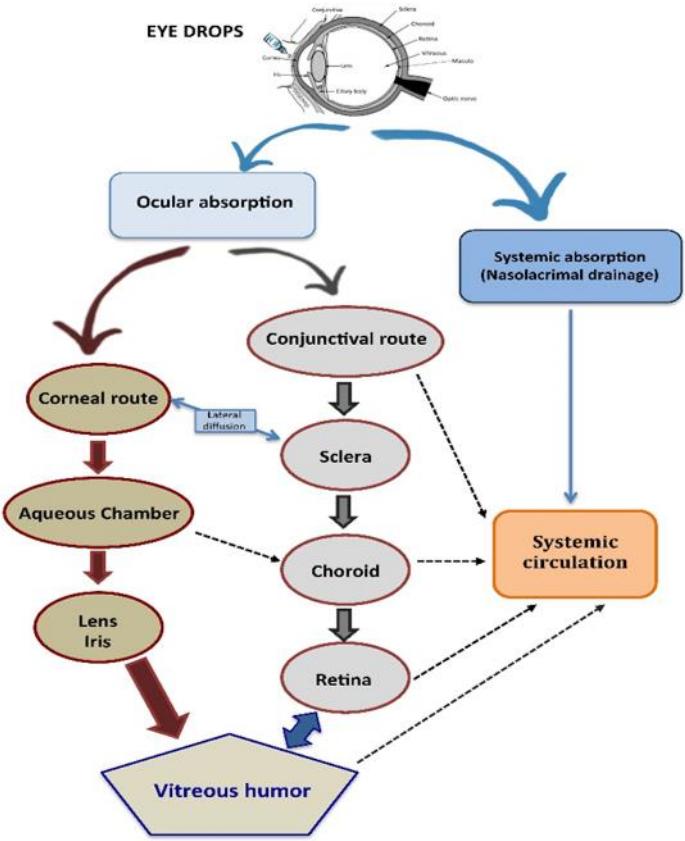

Fig. 3.2 Drug delivery to the eye. Following eye drop administration, drugs access the posterior segment by crossing the cornea or by non-transcorneal routes (*Modified from Tirassa et al., 2017*).

3.2 Effects of ed-NGF in eye and brain

The highly specialized structure of the retina makes this tissue vulnerable to a broad range of physical, chemical and pathological injuries. Vision is often considered as the most important of senses, and the one that most people fear losing. The leading causes of vision impairment and irreversible blindness are posterior segment related diseases (Pascolini and Mariotti, 2012), which include glaucoma, age-related macular degeneration (AMD), and diabetic retinopathy (DR) (Thrimawithana et al., 2011; Waite et al., 2017).
As stated above, NGF is a pleiotropic factor that extends its biological activity from the central and peripheral nervous systems to the endocrine, immune and visual system (Roberti et al., 2014). Following ocular injury, NGF and TrkA are expressed in the anterior segment of the eye (iris, ciliary body, lens, cornea, and conjunctiva), and NGF is released into the aqueous humor. Recently, it has been shown that NGF and its receptors are expressed also by the posterior segment, including choroid and retina (Lambiase et al., 2011). Experiments in rodents confirm the NGF actions on cornea cells, and the ability of ed-NGF administration to stimulate cornea innervation, epithelial cell healing, and corneal stem cells (Lambiase et al., 2012).
Recently, the safety and efficacy of ed-NGF has been also demonstrated in humans for the treatment of corneal degenerative diseases, such as neurotrophic keratitis and dry eyes (Sacchetti and Lambiase, 2014).
Neurotrophic keratitis (NK) is a rare and chronic degenerative corneal condition caused by a lesion of the trigeminal nerve, as well as by a corneal surgery and a complication of diabetes mellitus and multiple sclerosis (Lambiase et al., 2011). Treatment with ed-NGF induced a complete recovery of corneal ulcers associated with a significant improvement of corneal sensitivity and visual acuity (Aloe et al., 2008).
Experiments on patients and animal models of glaucoma and retina degeneration have also indicated ed-NGF as a noninvasive means to prevent retinal cell damage (Lambiase et al., 2011). Glaucoma is a term used to describe a group of conditions with a chronic and progressive optic neuropathy, characterized by gradual RGCs degeneration and morphological changes in the optic nerve with progressive deficit of the peripheral and central visual fields (Lambiase et al., 2010; Lambiase et al., 2011). It remains a leading cause of irreversible blindness throughout the world and one of the

most common neuropathies. Although the aetiology of glaucoma is still a matter of intense investigation, the risk factors for accelerated progression are: elevated intraocular pressure (IOP), age, thinner corneal thickness, vasculature dysregulation and genetic background (Almasieh et al., 2012).
Diabetic retinopathy (DR) is the most common form of diabetic eye disease. DR occurs in approximately one third of people with diabetes (Cheung et al., 2010; Olivares et al., 2017). It is the leading cause of blindness and results from changes in the vascular cells of the retina (Cuenca et al., 2014). Intravitreal and topical administration of NGF counteracts retina and optic nerve degeneration following bilateral carotid occlusions (Sivilia et al., 2009), and in models of diabetic retinopathy and glaucoma by reducing RGC loss and apoptosis (Colafrancesco et al., 2011). Visual functional recovery was also observed in patients with advanced glaucoma receiving ed-NGF for three months (Lambiase et al., 2009b). Furthermore, ed-NGF contrasts brain neurodegeneration in a rat model of diabetic encephalopathy induced by streptozotocin (STZ) by stimulating the survival of forebrain cholinergic neurons (Tirassa et al., 2013) and reducing the proNGF/p75NTR-induced apoptosis. Neuronal precursors in subventricular germinal area also respond to ed-NGF in diabetic brain by activating neurogenesis (Tirassa et al., 2015). Effects of ed-NGF in brain have also been demonstrated in acute experimental autoimmune encephalomyelitis (EAE) and diabetic rats, which represent models of inflammatory and dysmetabolic pathologies affecting respectively retina, optic nerve, and brain (Carito et al., 2015). Effects on forebrain are also reported in an acute EAE rat model, which re-produces the neuropathological and immunological symptoms of brain inflammatory diseases. Reduction in clinical signs and inflammatory markers was found in the frontal cortex, hippocampus and cerebellum of EAE rats receiving ed-NGF treatment, confirming the correlation between brain inflammation and disease manifestations, and supporting the proposed NGF anti-inflammatory effect (Waiczies et al., 2012).

CHAPTER 4
AIM OF THE PROJECT

NGF, the first discovered member of the neurotrophin family (Levi-Montalcini, 1987; Rosso et al., 2015), regulates neuronal cell functions, plasticity and repair in healthy and pathological conditions (Sofroniew et al., 2001). The NGF biological actions are mediated by two receptors: the NGF selective receptor TrkA, and p75NTR, which binds all neurotrophins, including the neurotrophin precursor forms (Chao and Hempstead, 1995; Davies, 1997). The interaction between p75NTR and proNGF induces apoptosis, and therefore favor neurodegeneration (Cuello et al., 2010), whereas survival is mediated by NGF/TrkA interaction (Cui, 2006). The safety and bioactivity of NGF applied on ocular surface as eye drops has been demonstrated in both humans and animal models, and successfully used for the treatment of ocular corneal ulcers (Lambiase et al., 1998; Aloe et al., 2008), but also suggested as a potential treatment for glaucoma, and retina (Lambiase et al., 2009a) and brain degeneration (Tirassa, 2011). Through the eye surface NGF reaches the retina, retinal projections, and different brain areas, including the cortex (Calza et al., 2011; Lambiase et al., 2011).
The results achieved in recent years on animal models and humans have shown that, similarly to endogenous NGF, ed-NGF acts on mature and precursor neuronal cells, activates differentiation and neurogenesis (Tirassa, 2011), and exerts protective and reparative activity in conditions of tissue damage also by modulating cytokines and growth factors (Carito et al., 2015).
The above evidence prompted us to further characterize and investigate the role of NGF in the regulation of neuronal cell survival in retina, optic nerve and brain, and to evaluate the effects of ed-NGF treatment in animal models of neurodegeneration.

In the first part of the project the unilateral optic nerve crush (ONC) model was used to investigate the changes in NGF signaling concurring to the retina degeneration. RGC degeneration following ONC has been extensively used as a model to study regenerative processes in the CNS (Aguayo et al., 1987; Bray et al., 1991; Benowitz and Yin, 2008), and to investigate the consequences of reduced retrograde support of growth factors, including NGF. RGC degeneration progresses even in the presence of a local increase of NGF. In glaucoma models, for example, retinal NGF is increased as early

as 7 days after crush (dac) (Rudzinski et al., 2004; Coassin et al., 2008). These findings indicate that enhancement of endogenous NGF levels is not sufficient to counteract neurotoxic mechanisms and support the survival of RGC (Coassin et al., 2008; Bai et al., 2010).

Whether the progressive RGC loss following optic-nerve injury might be related to dynamic changes in the expression of NGF and its receptors in the retina is not fully known. To study this question, a time-course study was performed to investigate the expression of NGF, proNGF and their receptors TrkA and p75NTR. In order to provide a mechanicistic explanation, the intracellular signaling pathways involved in ONC-related injury were also analyzed. Specifically, the evaluation of signaling pathways related to retinal cell stress and death, such as PARP (Poly (ADP-ribose) polymerase), caspase-3, p38, STAT1 and SAPK/JNK, crucial to identify critical temporal windows for neuronal recovery and treatment. Also, histological analyses were performed to monitor RGC survival and axonal damage during the experimental course. In addition, we extended the study to evaluate the effect of ocular administration of a topical formulation of recombinant human NGF (rhNGF) at 7 and 14 dac. Our working hypothesis was that administration of exogenous NGF during the first days after ONC might counteract and/or revert the intracellular events concurring to RGC death. The efficacy of intravitreal (ivt) and eye drops (ed) rhNGF in contrasting ONC-induced effects were firstly analyzed and compared by quantifying RGC loss and axon growth. Morphological and molecular analyses were extended through 14 dac to evaluate the ed-rhNGF dose effects on retina and optic nerve.

The second part of my Ph.D project focused on the effect of ed-NGF in diabetic retinopathy and encephalopathy using Streptozotocin (STZ)-induced diabetic rats as experimental model. DR, a major ocular complication of diabetes is characterized by progressive neuronal cell death (including RGCs degeneration), increased microvascular permeability, and enhancement in neovascularization due to increased production of pro-angiogenic factors such as vascular endothelial growth factor (VEGF), and its receptors VEGFR2 (Mysona et al., 2014). Furthermore, DR is characterized by an alteration in proNGF/NGF balance. Consistently, the observed increase in proNGF expression and the corresponding reduction in NGF production is responsible for the maintenance of neuronal and retinal function. This imbalance is accompanied by a concomitant variation of TrkA and p75NTR expression

levels. Based on this evidence, this experimental work evaluated structural damage and cell loss by means of biochemical approaches. Since ed-NGF interferes in the angiogenesis process, I analyzed the expression of VEGF and its receptor VEGFR2.

BDNF-related alterations in prefrontal cortex (PFC) are strongly associated with the onset of mood disturbances, such as depression and anxiety. ed-NGF stimulates BDNF in healthy retina and brain, suggesting that ocular NGF treatment might also be effective in regulating BDNF in pathological conditions. Thus, diabetic encephalopathy was also used to investigate the effects of diabetes and ed-NGF on BDNF and TrkB expression in prefrontal cortex.

Depressive phenotype was identified by force swimming test (FST). I comparatively evaluated the neurodegenerative effect of STZ in PFC using histological and immunofluorescence staining techniques. Protein extracted from prefrontal cortex were processed for biochemical analysis (ELISA and Western blot) to measure the expression of BDNF, proBDNF, TrkB and intracellular pathways.

Section II

RESULTS

CHAPTER 5
NGF SIGNALING IN THE RETINA OF ONC MODEL

The first main objective of my Ph.D project was to characterize intracellular pathways induced by optic nerve crush (ONC), including elements of NGF signaling pathway, and correlate them with morphological and functional changes in the retina and optic nerve.
Optic nerve crush (ONC) has been used as a model to analyze regenerative processes in the CNS, and investigate the consequences of reduced retrograde support of NGF.

5.1 Time-course of NGF and its receptors in ONC the retina

A time-course study was performed to characterize the expression of NGF, proNGF and their receptors, and intracellular pathways activated by ONC in the retina. Figure 5.1 shows the expression levels of NGF (measured by ELISA), proNGF, p75NTR and TrkA (evaluated by WB analysis) in the retina of control (CTR), CoEye (contralateral eye) and Crush groups (nerve-crushed eyes). No significant changes were found comparing the levels of each marker in the retina of CTR and CoEye groups at 1, 3, 7 and 14 days after crush (dac). In contrast, significant time-dependent variations were found in the Crush group compared to CTR and CoEye. A significant increase of NGF expression was found in the Crush retinas at 7 and 14 dac when compared to both CTR and CoEye, while no significant changes were detectable at 1 and 3 dac (Fig. 5.1 A). Similar results were obtained by WB analysis using a proNGF antibody (Fig. 5.1 B). A different trend was observed by analyzing the effect of nerve crush on the expression of NGF receptors. No significant changes of TrkA expression were found in the first week after crush, but a significant decrease in the Crush retinas was observed at 14 dac ($p<0.05$; Fig. 5.1 C). On the contrary, p75NTR levels started to increase significantly from the first dac and reached the highest levels at 14 dac (Fig. 5.1 D).

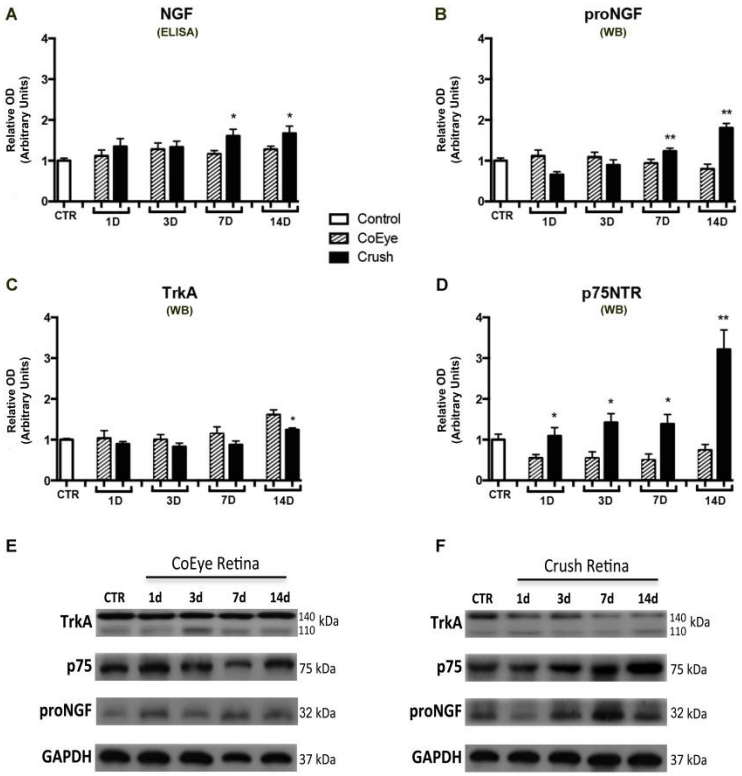

Fig. 5.1 Expression of NGF, TrkA and p75NTR in the retina from 1 to 14 dac. (**A-B**) Crush retinas had increased levels of NGF and proNGF at 7 and 14 dac. (**C**) TrkA expression was reduced in Crush retinas at 14 dac, while (**D**) p75NTR expression was increased in Crush retinas at all time points. (**E-F**) Representative images of the WB in CoEye and crushed retina respectively. Values are expressed as mean ± s.d *p<0.05, **p<0.01.

5.2 GFAP and p75NTR expression in the retina

WB analysis showed that GFAP levels were significantly increased following ONC (black bars) when compared to the CTR (white bar) and CoEye (bars with oblique lines) at the different time points. No changes in GFAP expression levels were observed in the CoEye retina when compared to CTR (Fig. 5.2).

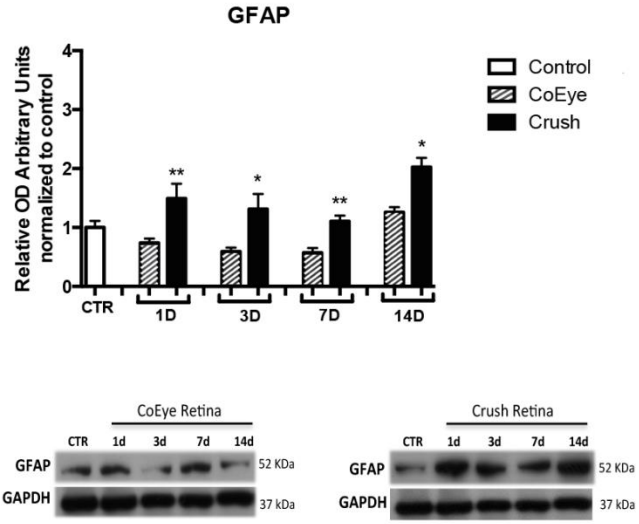

Fig. 5.2 Expression of GFAP in the retina 1 to 14 dac. GFAP levels was increased in the Crush retinas at all time points analyzed (n = 6 per group). Lower panels show representative images of the WB. * p<0.05, ** p<0.01.

Histological analysis confirmed the biochemical data showing an increased expression of GFAP at 14 dac. In the CoEye, $GFAP^+$ and $p75NTR^+$ cells were mostly confined to the ganglion cell layer (Fig. 5.3 A-B), while in the Crush

retinas both proteins were strongly expressed in the GCL and inner retinal layers (Fig. 5.3 D-E). GFAP$^+$ cell processes were distributed throughout the inner plexiform and nuclear layers (arrows in Fig. 5.3 D), indicating the presence of reactive astrocytes and increased GFAP expression in Müller cells. In addition, GFAP and p75NTR expression were often co-expressed in cells of the GCL (arrowheads in Fig. 5.3 F) and in Müller processes across the plexiform layers (arrows in Fig. 5.3 F), suggesting that retinal glial cells express this receptor.

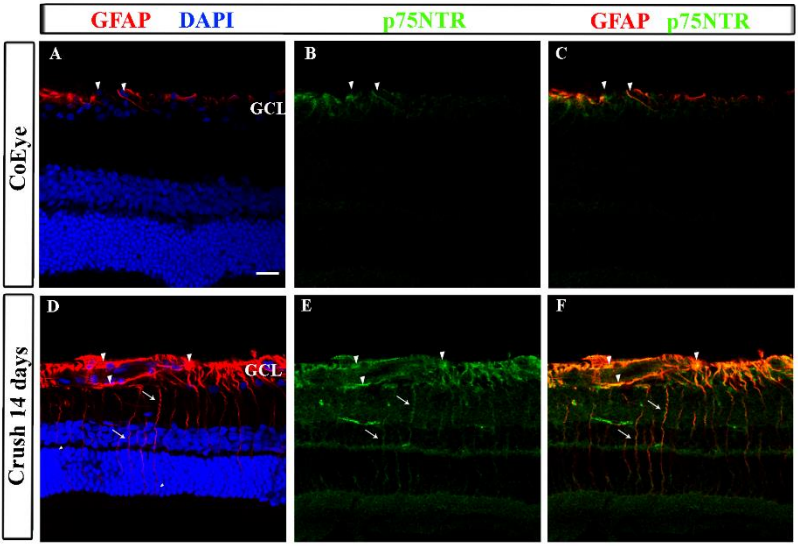

Fig. 5.3 GFAP and p75NTR expression in the retina 14 dac. (**A-B**) In the CoEye GFAP and p75NTR are expressed only in the GCLs. **(D-E)** In the Crush retinas, astrocytes in the GCL and Müller cells (arrows indicate radial processes) up-regulate GFAP and p75NTR. (**C-F**) GFAP and p75NTR merges. Arrowheads indicate cells that co-express GFAP and p75NTR.

5.3 Intracellular signaling in the retina

The activation of 18 signaling molecules in the retina was analyzed by a PathScan Intracellular Signaling Array Kit, which allows the detection of cellular proteins only when phosphorylated or cleaved at the specified residues. ERK1/2 (Thr202/Tyr2049) and BAD (Ser112) were phosphorylated in all samples, with no significant changes among the different groups. STAT3, S6 Rib Protein, HSP27, p70 S6 Kinase, p53 and GSK3 were not detectable in any of the samples, while STAT1, p38, SAPK/JNK and caspase-3 were activated only in Crush samples (Table 1).
The statistical analysis showed that optic-nerve crush significantly increased the retinal levels of STAT1, p38, SAPK/JNK, caspase-3 and PARP (Fig. 5.4).

Table 1. Intracellular pathway activation in the retina following ONC

Intracellular signals	CTR		1D		3D		7D		14D	
			CoEye	Crush	CoEye	Crush	CoEye	Crush	CoEye	Crush
ERK1/2	x	x	x	x	x	x	x	x	x	x
STAT1*				x		x		x		x
STAT3										
AKT (Thr308)					x	x[a]	x	x[a]	x	x
AKT (Ser473)				x[a]	x	x	x	x[a]	x	x
AMPKa			x	x	x	x	x	x	x	x
S6 Rib.Prot.										
mTor			x	x[a]	x	x	x	x[a]	x	x
HSP27										
Bad (Ser 112)	x	x	x	x	x	x	x	x	x	x
p70 S6 Kinase										
Pras 40			x	x[a]	x	x	x	x	x	x[a]
p53										
p38*				x		x		x		x
SAPK/JNK*				x		x		x		x
PARP*				x	x	x	x	x	x	x
Caspase 3*				x		x		x		x
GSK3										

The letter "x" indicates activation. The molecules with asterisk (*) in the "Intracellular signals" column were significantly activated by nerve crush, and the trend is shown in Fig. 5.4. The letter "a" indicates $p<0.05$ compared to CoEye.

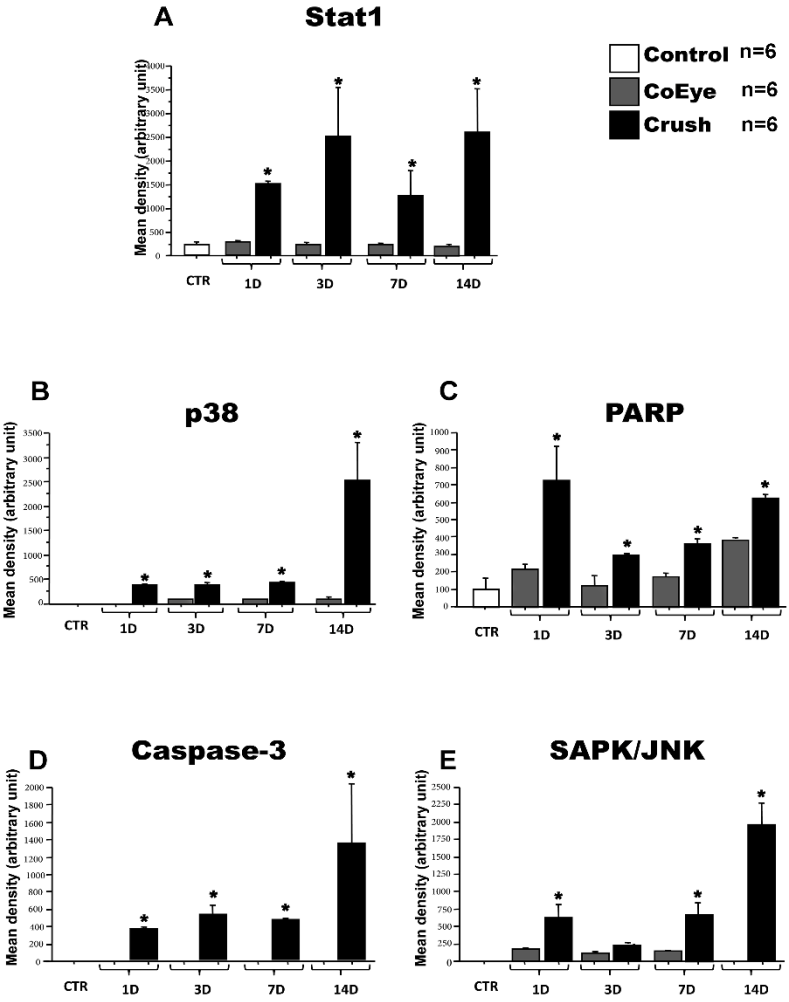

Fig. 5.4 Intracellular pathways modulated in the retina by crush at all time point analyzed. (**A**) STAT1; (**B**) p38; (**C**) PARP; (**D**) Caspase-3; and (**E**) SAPK/JNK. **p*<0.05 *vs*. CoEye.

5.4 Effects of ONC on the structural integrity of the retina

The effects of nerve crush on the distribution of RGC are shown in photomontages of retinal images (Fig. 5.5 A–C), which show several $Brn3a^+$ (green) nuclei and $Tuj1^+$ (red) cell bodies and axon bundles. While in the CoEye (Fig. 5.5 A) a large number of $Brn3a^+$ and $Tuj1^+$ cells (A', arrowheads) and axonal bundles (A, arrows) are visible, a progressive reduction of stained cells and axons is observable at 7 (Fig. 5.5 B) and 14 dac (Fig. 5.5 C, C', arrows and arrowheads).

The time-dependent effect of ONC on RGC survival was further demonstrated by quantitative analysis. At 7 dac, the number of $Brn3a^+$ cells in the central and peripheral retina was 50% of those detectable in the CoEye (Fig. 5.5 D), while $Tuj1^+$ cells were reduced by about 40% and 20% in the central and peripheral retina, respectively (Fig. 5.5 E). In accordance with the axon damage, a more dramatic reduction of RGCs was found at 14 dac, when the $Brn3a^+$ and $Tuj1^+$ cells were reduced by more than 80% in the central and peripheral retina respectively (Fig. 5.5 D–E).

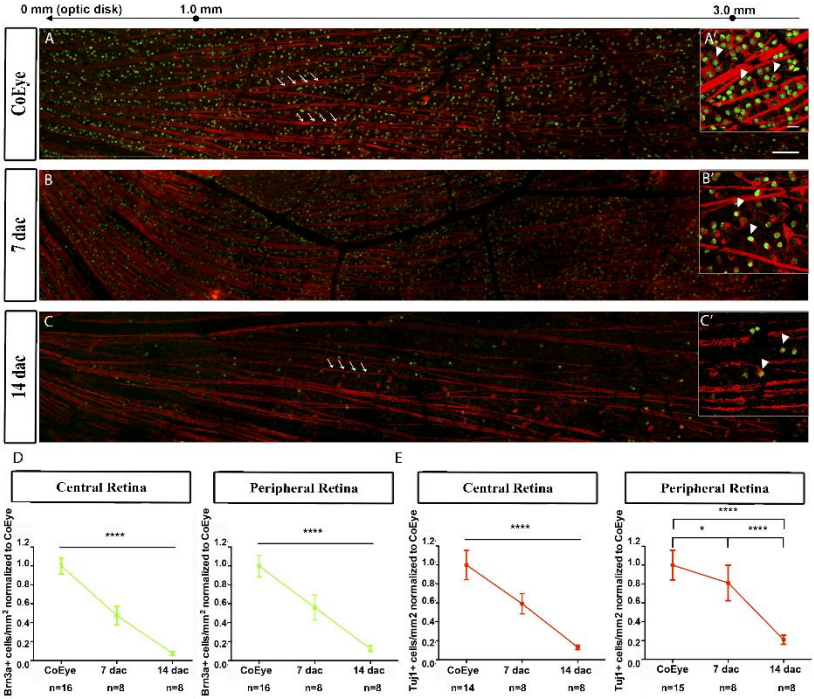

Fig. 5.5 Expression of Tuj1 (red) and Brn3a (green) in the retina at 7 and 14 days after crush (dac). (**A**) CoEye; (**B**) 7 dac; and (**C**) 14 dac. Arrows and arrowheads indicate axonal bundles and cell bodies, respectively; (**D**) Quantification of $Brn3a^+$ cells in the central and peripheral retina; (**E**) Quantification of $Tuj1^+$ cells in the central and peripheral retina. Scale bar: (**A**–**C**) 100 μm; (**A'**–**C'**) 20 μm. *p<0.05; ****p<0.0001.

CHAPTER 6
EFFECTS OF OCULAR APPLICATION OF NGF IN ONC MODEL RATS

As it will be discussed below, NGF signaling is altered following ONC. To support these results, we tested NGF potential effect on RGC survival and optic nerve regeneration by ocular NGF administration, by evaluating the morphological and biochemical effects of intravitreal (ivt) and topical (ed) application of human recombinant NGF (rhNGF) in an acute unilateral ONC model in adult rats.
The first set of experiment set investigates the retina at 7 dac, when about 50% of the RGC population is still present. The effects of ivt-rhNGF and ed-rhNGF administration on the eye are compared to treatment with vehicle to evaluate the efficacy of the different routes and doses of rhNGF ocular administration. Based on the results obtained in the first set, a second set of experiments was addressed to further investigate the survival effect of ed-rhNGF at 14 dac, when a large number of RGCs and their axons degenerate.

6.1 rhNGF intravitreal and topic delivery effects on RGC survival and axonal growth at 7 dac

The Tuj1 antibody was used to identify, in the flat-mounted retinas, RGCs in central and pheripheral retina**.**
Quantitative analysis shows that at 7 dac the percentage of $Tuj1^+$ cells in the crush eyes, respective to the CoEye, is reduced by about 50% in the central retina and 30% in the peripheral retina (Fig. 6.1 F and G). No significant changes are found by comparing ivt- and ed-vehicle treatments, indicating that the delivery route *per se* does not contribute to retinal cell death.
Treatment with rhNGF differently affected the number of RGCs in the central and peripheral retina. In rats receiving ivt-rhNGF, the percentage of Tuj1 cell loss in less than 20% in the central retina, resulting in ˜1.5 fold-increase with respect to vehicle-treated rats ($p<0.05$; Fig. 6.1 F and G). No significant

differences are found in the peripheral retina (Fig. 6.1 G). An increase in the percentage of Tuj1^{+} cells is also found in the rats receiving ed-rhNGF administration for 7 days. In the central retina only a small increase of RGC number is found in ONC rats receiving ed-rhNGF 180 treatment (p=0.06; Fig. 1.6 F), while the RGC number is similar to related CoEye following ed-rhNGF 540 (Fig. 6.1 F and G). A significant increase in RGC number is also found in peripheral retina of rats receiving ed-rhNGF 540 (Fig. 6.1 G).

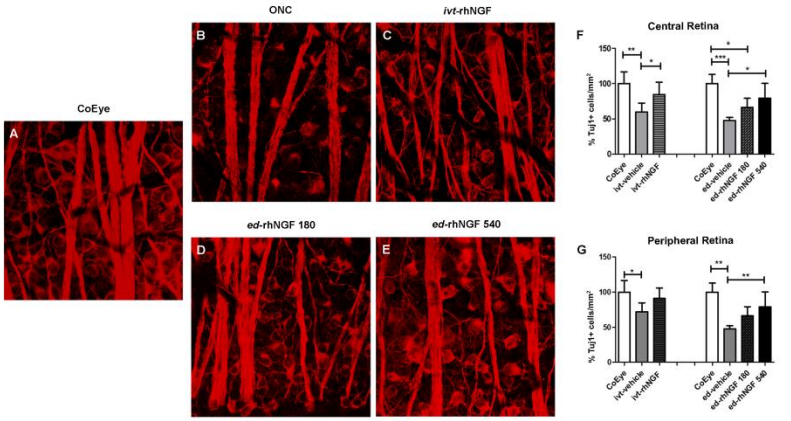

Fig. 6.1 RGC survival at 7 dac. (A-E) Tuj1 immunostaining on flat-mounted retinas. (G) The graph reporting the percentage of RGCs in the different groups. Both ivt-rhNGF and ed-rhNGF promote significant increase of RGC survival in the central retina (F), while only ed-rhNGF 540 effect peripheral RGC number (G). Statistically different *versus* CoEye: *p<0.05; **p<0.001; ***p<0.0001. Scale bar: 20 µm.

6.2 ed-rhNGF effects on RGC survival and axon growth at 14 dac

The effects of vehicle or ed-rhNGF administration on the distribution of Tuj1 positive cells in central retina is shown in a representative confocal image (Fig. 6.2 A-C). Compared to rats receiving vehicle, ˜ a 2- fold increase in the number of Tuj1^{+} cell is found in the central retina for both the ed-rhNGF 180 ($p<0.0001$) and ed-rhNGF 540 ($p<0.001$) treated groups (Fig. 6.2 D).

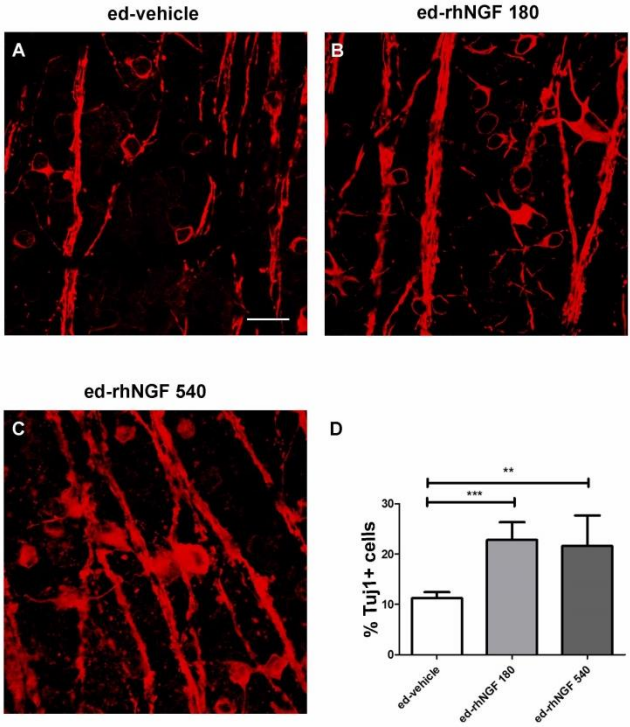

Fig. 6.2 ed-rhNGF effects on RGC survival at 14 dac. The pictures are representative images of Tuj1 stained cells in central retina of ONC rats receiving vehicle (A), ed-rhNGF 180 (B) and ed-rhNGF 540 (C). (D) The graph shown the percentage of RGCs in central retina. Statistically different *versus* CoEye: *$p<0.05$; **$p<0.001$; ***$p<0.0001$. Scale bar: 20 µm.

At 14 dac, RGC loss is associated with a decrease of axon regeneration in ONC rats. Very few axons express GAP-43 and cross the injury site in ONC rats receiving vehicle (Fig. 6.3 A), while numerous GAP-43^{+} cells are detectable in the nerve of ed-rhNGF treated rats (Fig. 6.3 B-C). Statistical analysis demonstrates a significant interaction between the treatment and the axon growth distance from the crush site (Fig. 6.3 D). A significantly higher number of axons at 0.25 mm from the crush site is seen in both ed-rhNGF 180 and 540 treated groups, but only in ed-rhNGF 540 at 0.50 mm distance (Fig. 6.3 D). No GAP-43 fibers are found at 1.5 mm after crush site in any of the experimental groups.

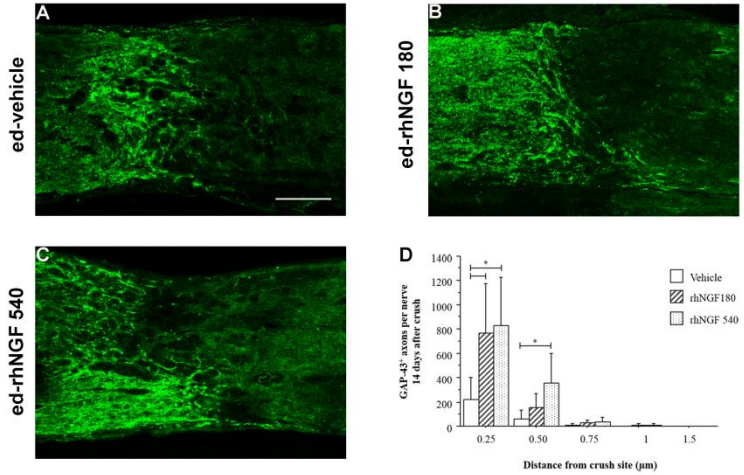

Fig. 6.3 ed-rhNGF effects on axon regeneration at 14 dac. Representative images of GAP-43 immunostaining an optic nerve of ONC rats receiving vehicle (A) or ed-rhNGF (B and C). The graph shows the number of GAP-43 fibers at increasing distances from the crush site in the various treatment groups (D). Statistically different *versus* CoEye: *p<0.05; **p<0.001; ***p<0.0001. Scale bar: 100 µm.

6.3 Nogo-A and p75NTR immunofluorescence in optic nerves at 7 and 14 dac

The decreased ability of mature RGCs to regrowth axons following ONC has been previously demonstrated to be dependent on the up-regulation and interaction between p75NTR and Nogo-A at optic nerve levels (Wang et al., 2002). Thus, we investigated the expression of these two markers at crush site following 7 and 14 dac in rats receiving vehicle or rhNGF treatment.
At 7 dac we observed a dense accumulation of p75NTR and Nogo-A positive cells at the crush site border in ONC rats (Fig. 6.4 A-B). Cells with or without processes co-expressing p75NTR and Nogo-A are also found in this area (Fig. 6.4 C). On the contrary, ONC rats receiving ivt- and ed-rhNGF present a reduced expression and different distribution of p75NTR (Fig. 6.4 D and G) and Nogo-A (Fig. 6.4 E and H). Although many cells expressing Nogo-A are detected, only few of them co-express p75NTR (Fig.6.4 F and I).

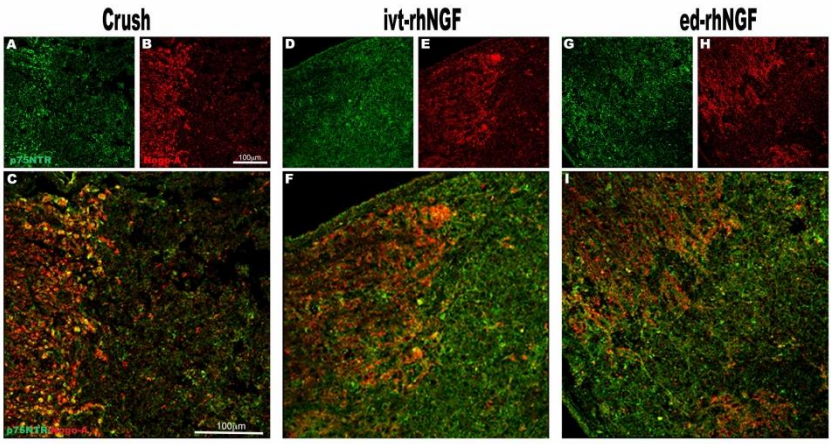

Fig. 6.4 p75NTR and Nogo-A expression in optic nerve at 7 dac. An increase in immunoreactive cells expressing p75NTR (A) and Nogo-A (B), and co-expressing the two markers (C) was detected at the proximal border of the crush site in ONC+vehicle rats. Staining of both p75NTR (D,G) and Nogo-A (E,H) were differently distributed in ONC+rhNGF groups, showing a reduced p75NTR staining and a decrease of p75NTR/Nogo-A cells of ivt- and ed-rhNGF (F,I). Scale bar in white: 100 µm.

At 14 dac a more visible central unstained area delimited by intense p75NTR and Nogo-A immunoreactivity is recognisable in the ONC+vehicle group (Fig. 6.5 A-C). The z-stack analysis confirms that p75NTR and Nogo-A are co-expressed at both margins of the crush site, and an accumulation of double stained cells are present in the area proximal to the nerve head (see arrow in Fig. 6.5 C). The central zone of the crush site are also presents cells and fibers expressing p75NTR surrounded by Nogo-A immunoreactive spots (Fig. 6.5 G). Moreover, cells co-expressing p75NTR and Nogo-A are found at both the proximal and distal borders of the crush site (Fig. 6.5 H).
The major difference found by comparing the distribution of the two markers at the crush site in ONC+vehicle and ONC+ed-rhNGF is the marked reduction of p75NTR immunoreactivity (Fig. 6.4 D). Indeed, while no appreciable changes are found in the expression of Nogo-A (Fig. 6.5 E), few cells are positive for p75NTR, and no coexpression of the two markers is observable at optic nerve crush level of rats receiving ed-rhNGF (Fig. 6.5 F). The z-stack analysis confirms that only occasional cells/fibers express p75NTR and Nogo-A with respect to what is found in the vehicle treated rats.

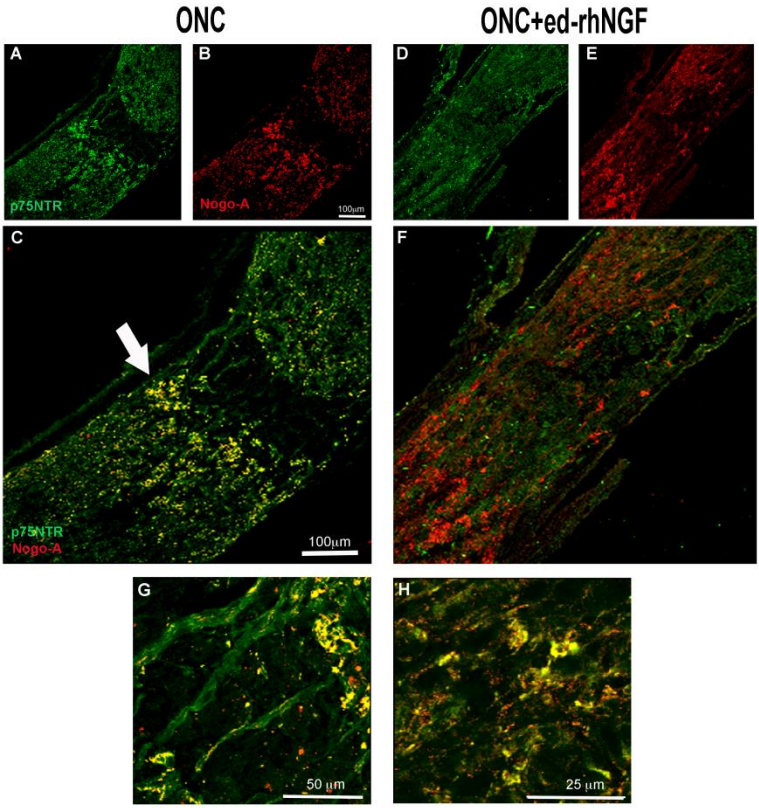

Fig. 6.5 p75NTR and Nogo-A expression in optic nerve at 14 dac. Distribution of p75NTR (A) and Nogo-A (B) immunoreactivity was found at the crush site of ONC+vehicle. (C) p75NTR/Nogo-A costaining was still present at the crush site. A marked reduction of p75NTR staining was observed at the crush site of ONC rats receiving ed-rhNGF (D), while Nogo-A distribution appears similar to what found in ONC+vehicle (E). Scale bar in white:100 µm; Magnification: 50 and 25 µm.

6.4 proNGF and NGF receptor expression and activation in the retina

No significant differences are found when comparing the expression levels of proNGF, TrkA and p75NTR in CTR and CoEye of ONC group at 7 and 14 dac, even following ed-rhNGF treatment on the left eyes.
The post hoc analysis reveals a significant increase in expression levels of proNGF and p75NTR in the ONC retina at 7 and 14 dac, while no TrkA reduction is found at 14 dac (Fig. 6.6 A-D). Compared to ONC receiving vehicle, a reduction of proNGF and p75NTR levels is found, at the two time points considered, when ed-rhNGF was administered at the doses of 180 and 540 µg/ml (Fig. 6.6 A and B respectively). No variation in TrkA is also found at 7 dac, while a significant increase of TrkA levels is observed at 14 dac but only following application of ed-rhNGF 540 µg/ml (Fig. 6.6 C).

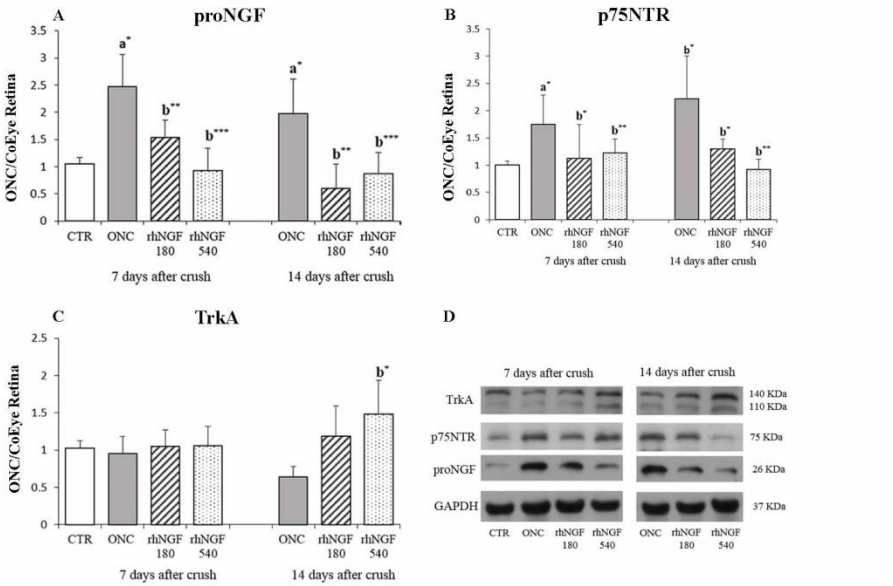

Fig. 6.6 NGF receptor and proNGF expression levels in retina at 7 and 14 dac. The graphs show proNGF (A), p75NTR (B) and TrkA (C) expression in the left (ONC) and the right (health) retina at 7 and 14 dac. (D) Shows representative WB analysis. Values are expressed as mean of ONC/CoEye ± s.d. Statistically different: **a** *vs* CTR; **b** *vs* ONC. **p*<0.05, ***p*<0.01, ***p<0.0001.

At the same time points, the effects of ONC and ed-rhNGF on the phosphorylation levels of TrkA were also evaluated. No differences in pTrkA is found in all CoEye groups and in the crushed retina of ONC+vehicle, while independently of the dose used, an increase of pTrkA/TrkA is found in the ONC+rhNGF retina when compared to both CTR and ONC+vehicle (Fig. 6.7 A). Similar results are obtained by analyzing the expression and phosphorylation levels of ERK 1/2 at 14 dac. No significant variation was found in total ERK expression in all experimental groups, while treatment with rhNGF significantly increase ERK phosphorylation when administered at 540 µg/ml ($p<0.0001$ *vs* ONC+vehicle) (Fig. 6.7 B and E).
No significant changes of the levels of total and phosphorylated AKT are found in any rats groups (Fig. 6.7 C and F).

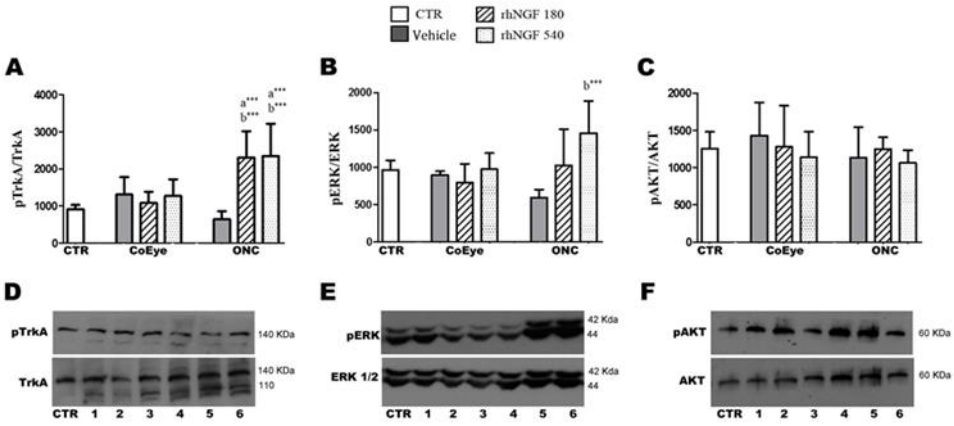

Fig. 6.7 TrkA and intracellular signal phosphorylation. The phosphorylation levels of p-TrkA, ERK 1/2 and AKT were analyzed and compared to the expression of their total unphosphorylated form in the CoEye and crushed retina of ONC and ONC+ed-rhNGF at 14 dac. Values are expressed as mean ± s.d. Statistically different: **a** *vs* untouched and untreated rats (CTR); **b** *vs* ONC+vehicle;. *p<0.05, **p<0.001, ***p<0.0001.

CHAPTER 7
EFFECTS OF ed-NGF IN STZ-INDUCED DIABETIC RATS

To gain further insights into the role of NGF in the protective mechanism of RGC degeneration, in the second part of my study we investigated the effect of ed-NGF administration on retina and brain of rats with experimentally induced-diabetes.

The present study investigates structural modifications of RGCs and biochemical changes of NGF-receptors and VEGF signaling in the retina.

Western blot was used to analyze the expression levels of NGF receptors in the retina. p75NTR FL (full length) was significantly increased ($p<0.05$) in diabetic retina compared with CTR rats (Fig. 7.1 A). Interestingly, the endogenous intracellular domain fragment of p75NTR (p75ICD) was also produced in the retina and, as well as p75NTR FL, increased in STZ rats when compared to CTR group ($p<0.01$). ed-NGF administration did not induce changes in retinal p75NTR FL levels from STZ and STZ+NGF-treated animals. On the contrary, ed-NGF mediates a further increase in p75ICD when compared to CTR and STZ groups (Fig. 7.1 A). Furthermore, a significant increase in proNGF protein levels was found in STZ retina when compared to CTR ($p<0.05$), and ed-NGF treatment is able to properly restore proNGF basal levels (Fig. 7.1 B).

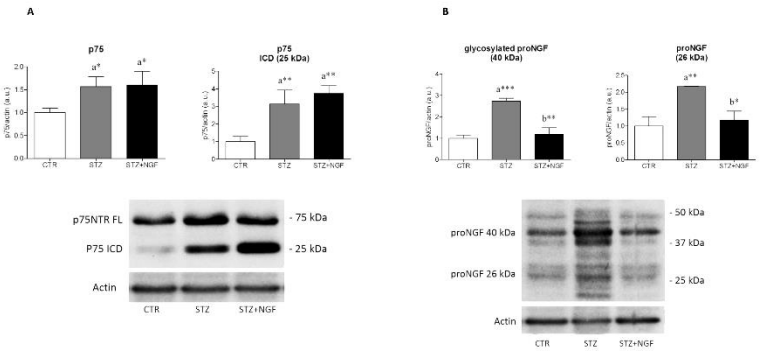

Fig. 7.1 p75NTR and proNGF expression levels in the retina. The graphs show p75NTR (A), proNGF (B) levels of CTR, STZ and STZ+NGF groups. Statistically different: **a** *vs* CTR; **b** *vs* STZ. *p<0.05, **p<0.001, ***p<0.0001.

The analysis of TrkA expression showed a significant decrease in STZ rats with respect to CTR animals, while ed-NGF administration restored TrkA levels in the retina (Fig. 7.2).

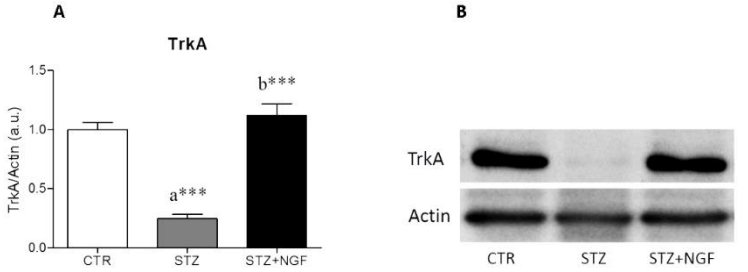

Fig. 7.2 Expression levels of TrkA in the retina. (B) Shows representative WB analysis. Statistically different: **a** *vs* CTR; **b** *vs* STZ. ***p<0.0001.

Experimental evidence indicates the existence of a regulatory interplay between NGF and VEGF signaling. As VEGF is one of the major growth factors involved in the induction of deleterious neoangiogenesis in DR, we also evaluated the prospective effect of ocular NGF treatment on VEGF pathway. ed-NGF efficiently counteracted the rise in VEGF expression observed in STZ retinas. VEGFR2 expression showed an opposite trend if compared to its ligand, being dramatically reduced in STZ-treated rats and restored to CTR levels upon ed-NGF administration (Fig. 7.3).

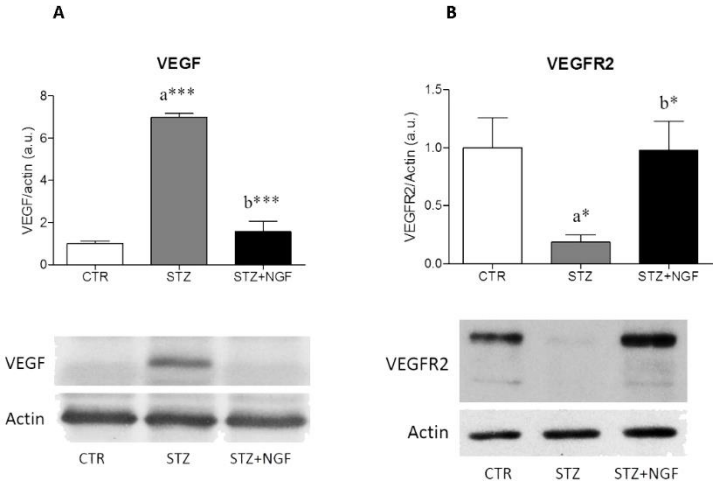

Fig. 7.3. Expression levels of VEGF and VEGFR2 in the retina. (B) Shows representative WB analysis. Statistically different: **a** *vs* CTR; **b** *vs* STZ. *p<0.05, ***p<0.0001.

CHAPTER 8
ed-NGF MODULATES BDNF IN PREFRONTAL CORTEX OF DIABETIC RATS

Neuronal and axonal loss following STZ is not limited to cholinergic brain areas, but it has been reported in PFC in developing and adult rodents (Castillo-Gomez et al., 2015). Altered myelination and plasticity in PFC is associated with the manifestation of depressive phenotype following diabetes, and suggested to be dependent on changes in BDNF signaling (Katon, 2008). Reduced levels of BDNF are found in the serum of STZ rats (Tirassa et al., 2012), but whether diabetes also induces alteration of BDNF in PFC has not been fully investigated previously. To address this question, a study was carried out to evaluate the effects of diabetes and the expression of BDNF, its intracellular signaling molecules in PFC and possible relationship with neurobehavioral changes in STZ-induced diabetic rats treated or not with ed-NGF (see Supplementary Chapter of Material and Methods for details).

This study confirms the neurodegenerative effect of diabetes in PFC by showing altered distribution of neuronal cells in the cingulate cortex (Cg1) and motor cortex (M1) of STZ rats (Fig. 8.1 D–F) when compared to the healthy rats (Fig. 8.1 A–C). With respect to PFC, our study shows a loss of neurons - demonstrated by the reduction in cells expressing NeuN - in all the cortical layers of STZ rats (Fig. 8.1 I) compared to CTR rats (Fig. 8.1 G), and especially so in layers II and III, where the presence of cleaved caspase-3 was also detected (Fig. 8.1 M-N). Cells expressing glutamic acid decarboxylase 67 (GAD67) in layers V-VI were also affected in STZ PFC (Fig. 8.1 L), compared with CTR (Fig. 8.1 H) as demonstrated by an increased colocalization of GAD67 and cleaved caspase-3 (Fig. 8.1 O-P and P'). These specific diabetes-induced alterations in PFC were associated with changes in BDNF signaling and related behavioral manifestations, as described below.

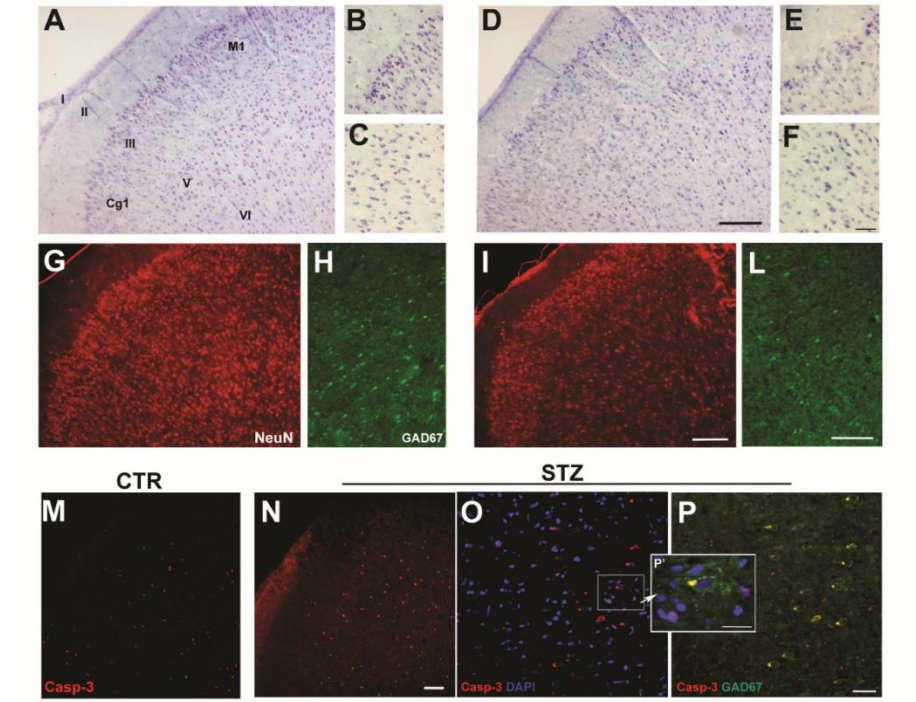

Fig. 8.1 Morphological evidences of the STZ-induced neuronal alterations in PFC. Cell loss is observed in the cingulate cortex (Cg1) and motor cortex (M1) of STZ rats (D–F) when compared to the healthy rats (A–C). Altered distribution of cells expressing NeuN is found in all the cortical layers of STZ rats (I) with respect to CTR rats (G). Compared with CTR (H), STZ also affected the expression of GAD67 in layers V-VI of PFC (L). Stain for cleaved caspase-3 (Casp-3) in the Cg1 and M1 areas of CTR and STZ PFC is shown in panels M and N, respectively. Magnifications in figure O, P, and P' (Scale bars: 20 µm) confirm the presence of apoptosis in both GAD67 cells (yellow stain), and in no GABAergic small cells in the PFC of diabetic rats. Scale bars: 50 µm.

8.1 Effects of STZ and ed-NGF on body weight and behavior

Compared with the other groups, a significant body weight reduction was observed in STZ rats. This significant reduction started from 5 weeks days post induction (dpi), while a recovery was observed following ed-NGF treatment ($p=0.05$; Fig. 8.2 A).
Concerning the effects of treatment on behavior, a multicomparative analysis shows that diabetes induces a depressive phenotype, which is partially recovered by treatment with ed-NGF. Indeed, a significant reduction in first floating latency during forced swim test (FST) in STZ group compared with healthy controls was found (Fig. 8.2 B; $p<0.05$ *vs*. CTR and CTR+NGF). A significant increase in latency time was observed in STZ+NGF animals when compared to the diabetic group. Indeed, while STZ rats showed about 2-min latency, the ed-NGF group displayed immobilization after a 3-min latency time ($p<0.05$). No significant differences were observed between STZ+NGF and CTR or CTR+NGF (Fig. 8.2 B).

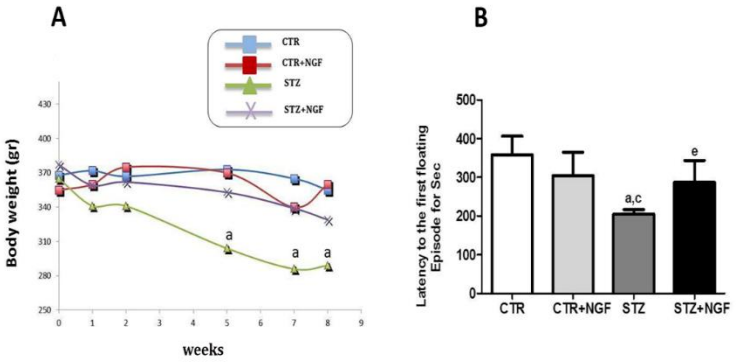

Fig. 8.2 Effects of STZ and ed-NGF on body weight. (A) and on first floating latency by forced swim test (B). Statistically significant changes: **a** $p<0.05$ *vs* CTR; **c** $p<0.05$ *vs* CTR NGF; **e** $p<0.05$ *vs* STZ.

8.2 Effect of ed-NGF on BDNF and its receptors

Unchanged BDNF levels were found comparing healthy and STZ rats, even when receiving NGF treatment (Fig. 8.3 A). WB analysis shows about a 2-fold increase in proBDNF in the PFC of STZ when compared to CTR ($p<0.05$) and STZ+NGF ($p<0.05$). Levels of proBDNF in CTR+NGF were similar to controls (Fig. 8.3 B).

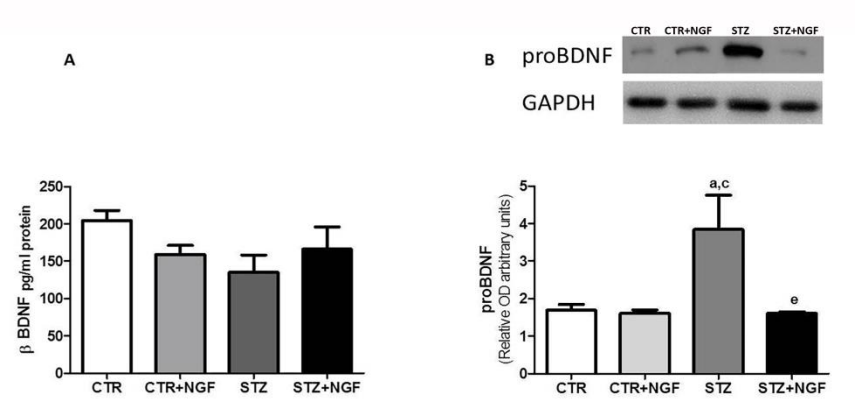

Fig. 8.3 The effects of diabetes and ed-NGF on the BDNF (A) and proBDNF (B) in prefrontal cortex. A representative WB is shown in the upper panel of B. Statistically significant changes: **a** $p<0.05$ *versus* CTR; **c** $p<0.05$ *versus* CTR + NGF; **e** $p<0.05$ *versus* STZ

STZ and NGF significantly affect the expression of both p75NTR and TrkB. Diabetic rats show increased p75NTR and decreased TrkB expression levels, while treatment with ed-NGF results in normalization of STZ-induced changes. A significant increase in p75NTR was also found in healthy rats receiving treatment with ed-NGF when compared to respective controls (Fig. 8.4 A). Treatment with ed-NGF also enhanced TrkB expression in both CTR ($p<0.01$) and STZ rats ($p<0.05$), while a reduction was found in the PFC of diabetic rats (Fig. 8.4 B). Evaluation of the individual TrkB/p75NTR expression ratio confirms the different effects of diabetes and ed-NGF showing that STZ induces unbalanced BDNF receptor expression, favoring p75NTR. A different trend is observed in healthy and STZ rats receiving ed-NGF in which the ratio between the two BDNF receptor types is enhanced (Fig. 8.4 C). To analyze TrkB activation, its phosphorylation levels were measured by ELISA. Multicomparative analysis shows that p-TrkB is decreased in STZ ($p<0.01$), and in both CTR and STZ rats receiving ed-NGF ($p<0.05$ and $p<0.01$, respectively) compared with healthy control rats. A significant increase ($p<0.05$) was found in p-TrkB level in the PFC of STZ+NGF rats when compared to STZ (Fig. 8.4 D).

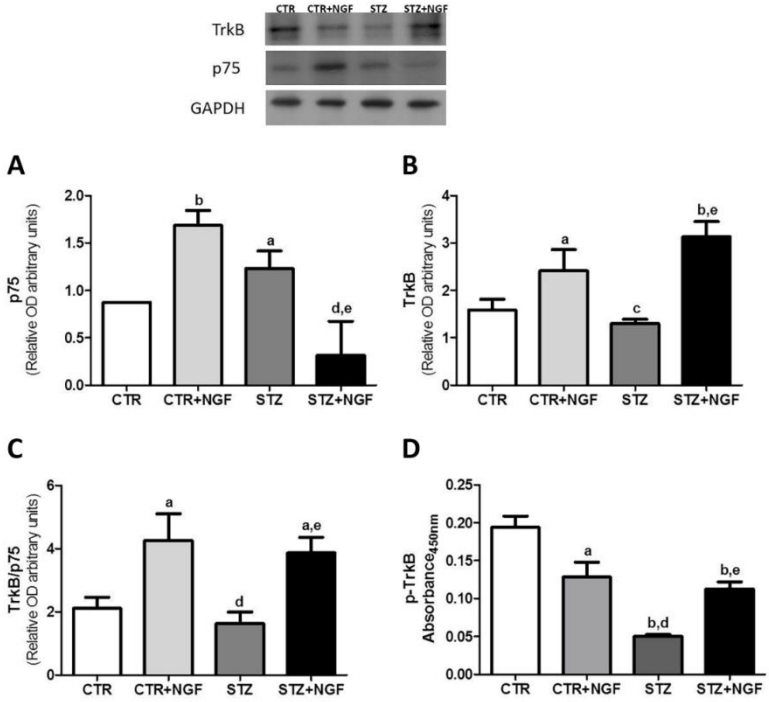

Fig. 8.4 Expression of p75NTR and TrkB in prefrontal cortex of CTR and STZ rats. The top panel shows a representative WB for BDNF receptors. (C) reports the graph of TrkB/p75NTR ratio in the PFC of the different rat groups. (D) The p-TrkB levels were measured by ELISA. Statistically significant changes: **a** $p<0.05$ and **b** $p<0.01$ *versus* CTR; **c** $p<0.05$ and **d** $p<0.01$ *versus* CTR+NGF; **e** $p< 0.05$ *versus* STZ.

8.3 Correlation between FST latency and BDNF

A simple regression analysis was performed to identify a possible correlation between the manifestation of a depressive mood and changes in the expression of BDNF and its receptors. No significant correlation was found between the latency time (dependent variable) and expression levels of BDNF, p75NTR, and TrkB (data not shown), while proBDNF and p-TrkB correlated significantly with this FST parameter. Indeed, an inverse (proBDNF) and direct (p-TrkB) correlation with the FST immobilization time measured in the experimental was found (Fig. 8.5 A and B). Similarly, when the depression phenotype is manifested, the levels of proBDNF and p-TrkB are increased and decreased, respectively.

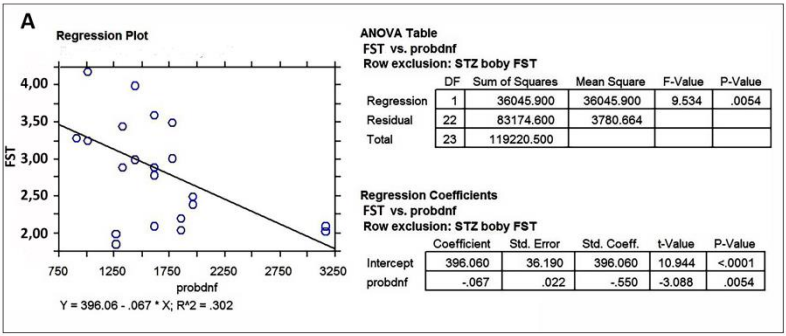

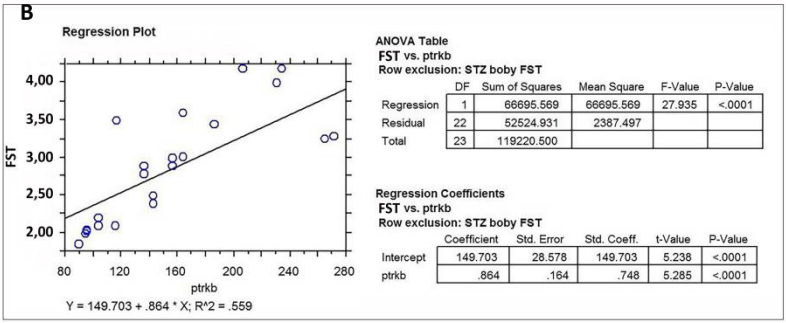

Fig. 8.5 Correlation between FST immobilization time and the PFC expression of proBDNF (A) and p-TrkB levels (B). p-TrkB levels are positively correlated with the FST immobilization time ($p<0.01$), while a negative correlation was found for proBDNF ($p=0.0054$).

8.4 Effects of STZ and ed-NGF on BDNF intracellular signals

WB analysis was used to measure the effects of STZ and NGF on the expression levels and phosphorylation of two major downstream signaling molecules, Akt and SAPK/JNK (Fig. 8.6). Compared with CTR, a decrease of about 80% of phosphorylated Akt (p-Akt) levels was found in STZ PFC, but a significant reduction was also found in CTR + NGF (about 50%) and STZ + NGF (about 45%) (Fig. 8.6 B). When the relative individual ratio of p-Akt/Akt was considered, a significant decrease was found in both STZ and STZ + NGF, but not in CTR + NGF (Fig. 8.6 D).
Moreover, STZ rats showed no significant variation of phosphorylated JNK (p-JNK) levels when compared to CTR, while treatment with ed-NGF in healthy and diabetic rats caused a significant decrease in p-JNK levels ($p<0.01$; Fig. 8.7 B). No changes were found in the levels of total JNK (Fig. 8.7 C), and thus, the p-JNK/JNK ratio confirms the effects of STZ and ed-NGF on the phosphorylation levels of both JNK isoforms (46 kDa and 54 kDa).

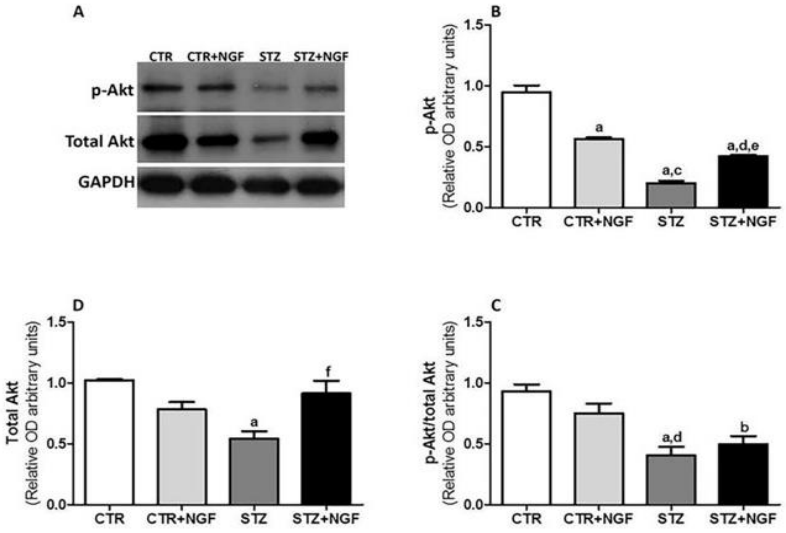

Fig. 8.6 The effects of diabetes and ed-NGF treatment on the expression levels of p-Akt and Akt are shown in the representative Western blot (A) and graph (B–D). The ratio between p-Akt and total Akt protein expression is shown in the graph of D. Statistically significant changes: **a** $p<0.05$ and **b** $p<0.01$ *versus* CTR; **c** $p<0.05$ and **d** $p<0.01$ *versus* CTR + NGF; **e** $p<0.05$ and **f** $p<0.01$ *versus* STZ.

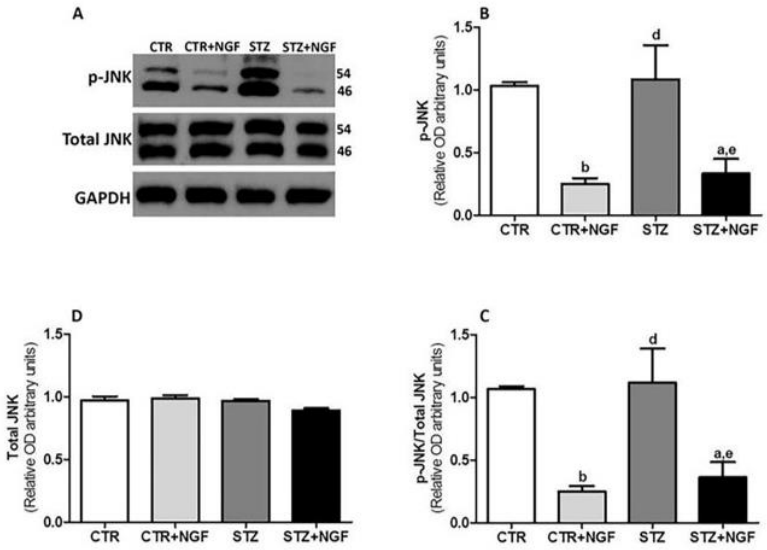

Fig. 8.7 The representative Western blot image of JNK is shown in A, note two bands at 46 kDa and 54 kDa corresponding to the JNK1 isoform, and the unseparated JNK2 and three isoforms, respectively, in their phosphorylated and no phosphorylated state. The WB quantification analyses of the p-JNK and total JNK in PFC in the different rat groups are reported in B and C. The ratio between p-JNK and total JNK protein expression is shown in D. Statistically significant changes: **a** $p<0.05$ and **b** $p<0.01$ *versus* CTR; **c** $p<0.05$ and **d** $p<0.01$ *versus* CTR + NGF; **e** $p<0.05$ and **f** $p<0.01$ *versus* STZ.

The caspase-3 expression level was significantly higher in STZ rats (STZ=1.242±0.14 relative OD^{450} ± s.d.; $p<0.01$) compared with CTR (CTR=0.946±0.052) and STZ + NGF (STZ+NGF=0.618±0.168; $p<0.01$). No significant changes were found in CTR + NGF (=0.782±0.123) and STZ + NGF when compared with CTR group (data non shown).

Section III

DISCUSSION AND CONCLUSIONS

CHAPTER 9
DISCUSSION AND CONCLUSIONS

9.1 Role of endogenous and exogenous NGF in the injured retina

In recent years, increasing evidence shows that NGF administration as eye drops on the ocular surface (ed-NGF) reaches the retina and the optic nerve at doses sufficient to induce biological effects. In addition, the eye-brain pathway is responsible for the delivery of ed-NGF to some brain areas, offering a new potential approach to study NGF's role not only in ocular pathologies, but also in brain disorders.

The purpose of my Ph.D. project was to investigate the role of NGF in the animal models of ONC, and diabetes retinopathy and encephalopathy induced by STZ injection. To reach this aim, we used a pharmacological approach based on ed-NGF administration to evaluate the potential roles of this molecule in different ocular and brain physiopathological conditions.
The results of my studies confirm that ONC induces 50% and 80% of RGCs loss at 7 and 14 dac, respectively. The time course analysis showed a rapid activation of apoptotic pathways, which were associated with a fast enhancement of GFAP.
Furthermore, similarly to what has been observed in glaucoma models (Rudzinski et al., 2004; Coassin et al., 2008), we found that ONC-induced retina degeneration is triggered and/or exacerbated by an imbalance between the Trk-mediated survival and growth actions, and p75NTR-mediated activation of apoptosis/growth inhibitory pathways. The same results were obtained in the retina of STZ rats, in which we observed a significant increase of p75NTR and proNGF in diabetic rats with a concomitant significant decrease of TrkA levels. These findings support the concept that endogenous NGF is not sufficient to protect RGCs following injury.
Thus, we hypothesized that increased availability of mature NGF at the retinal level might be neuroprotective by favouring survival/growth pathways. To validate this hypothesis, we investigated the effects of ocular treatment with mature NGF in early retina post-injury stage. We found that ed-NGF promoted RGC survival and regeneration by suppressing the

activation of the pro-apoptotic pathway in retina and optic nerve. The NGF anti-apoptotic effects were accompanied by increased TrkA activation, and reduced proNGF/p75NTR expression.

Amhed and colleagues (Ahmed et al., 2006) demonstrated survival and regenerative effects of intravitreal administration of sciatic nerve-derived Schwann cells, which secrete growth factors including NGF. In line with this study, our results show that mature NGF increases at the retinal level, promoting p75NTR cleavage. In addition, we found that, in parallel with p75NTR FL reduction, ed-NGF also stimulates proNGF cleavage resulting in reduced levels of its active form (26 kDa). The shift from survival to degeneration is favoured by the increase of proNGF levels with respect to the mature form, which might depend on a reduced maturation of the NGF precursor, or on an accelerated degradation of the mature neurotrophin (Davies, 1997). Thus, in agreement with these two studies, we suggest that ed-NGF might inhibit apoptosis by affecting p75NTR and its pro-apoptotic ligand proNGF, resulting in an increase of RGC survival.

RGC survival induced by ed-NGF is associated with enhanced of VEGFR2 levels. Since VEGFR2 expression is particularly abundant in retinal neurons, this increase allows the receptors to bind and whelm VEGF, which is secreted around neurons in physiological conditions. When this event is impaired, for instance during RGC loss, as we have observed in diabetic rats, the contributory reduction in VEGFR2 impedes VEGF titration by neurons. Thus, the subsequent rise in VEGF around neurons can cause a misdirected angiogenic process (Okabe et al., 2014).

Moreover, we found increased levels of p75ICD in the degenerating retina, and a further build-up following ed-NGF. It has been demonstrated that p75ICD possesses both the ability to induce apoptosis and survival as a function of cellular context. When TrkA expression is low, it preferentially induces apoptotic pathways; on the other hand when TrkA is highly co-expressed, p75ICD potentiates TrkA activity thus favouring growth and survival (Matusica et al., 2013). In our experimental conditions, it is likely that in degenerating retina, where TrkA levels are strongly reduced, p75ICD induces cell death. Following ed-NGF administration, the increase in p75ICD and the contributory restoration of TrkA levels could instead promote neuroprotective effects. Besides the potential p75ICD-mediated enhancement of TrkA, ed-NGF might also exert a neuroprotective effect by directly binding to TrkA through the classical mechanism of activation.

Besides effects on the retina, we found that ed-NGF also affects the molecular pathways involved in axonal growth after optic nerve damage. Several reports demonstrated that this process is strongly influenced by p75NTR (Mesentier-Louro et al., 2017). Indeed, once stimulated by Nogo-A, Nogo-R interacts with p75NTR and activates RhoA/Rock signaling cascade, thus leading to cone growth collapse and axonal growth blockade (data not included in this thesis).
Morphological analysis showed that ocular rhNGF administration to cause changes of Nogo-A and p75NTR distribution at the crush site at both 7 and 14 dac. At 7 dac, following ONC, p75NTR and the Nogo-A increase at the crush site in reactive glial cells forming the scar inhibits axon growth, as already reported (Yiu and He, 2006). At 14 dac, Nogo-A and p75NTR co-localization is high at both crush borders. Treatment with ed-NGF results in a different p75NTR expression and distribution at the nerve level. On the contrary, Nogo-A is slightly affected by ed-NGF treatment. Overall, the suppression of cell infiltration at crush site at 7 dac, and the reduced p75NTR expression at 14 dac following ed-NGF suggest, for the first time, that the treatment impedes glial scar formation and facilitates axonal regrowth.
These observations are in line with previous reports, and suggest that ed-NGF reduces p75NTR, and potentially impairs its binding with Nogo-R. This event could represent the molecular mechanism by which ed-NGF stimulates axon regeneration. Moreover, the fact that ed-NGF reaches the optic nerve suggests that NGF treatment is able to exert effects also in brain visual areas, such as visual cortex and lateral geniculate nucleus.
Consistent with this notion, ongoing studies in our laboratory support this hypothesis, showing that ONC leads to deregulations in TrkA and p75NTR expression in superior colliculus, lateral geniculate nucleus and visual cortex. These alterations are accompanied by a functional reduction in glutamatergic transmission. Importantly, ed-NGF treatment counteracts the degenerative features induced by ONC (unpublished data).

In summary, these studies confirm that NGF is a crucial factor for the structural and functional maintenance of visual system, and that degenerative events occurring in DR and ONC are caused, at least in part, by unbalances in NGF signaling. The biochemical and functional recovery observed after ed-NGF treatment suggest that modulation of NGF pathway could represent a valuable pharmacological approach for the management of several neurodegenerative conditions.

9.2 Involvement of BDNF signaling in ed-NGF effects in brain

Our study confirms that ed-NGF exerts effects in the pathological brain and suggests a potential mechanism of action of ed-NGF treatment by demonstrating modulation of BDNF signaling in prefrontal cortex and the recovery of STZ-induced FST immobilization time.

Firstly, our study shows that the levels of proBDNF and TrkB phosphorylation are correlated with immobilization latency In STZ rats we demonstrate that changes of BDNF signaling in PFC might be markers of a depressive phenotype. Further, showing that treatment with ed-NGF is able to recover both the biochemical and behavioural STZ-induced alterations supports its ability to modulate brain BDNF, and suggests a possible mechanism of actions.

Specifically, we found increased levels of proBDNF and p75NTR and enhanced caspase-3, while phosphorylation of TrkB and AKT were reduced in the PFC of STZ rats. These data suggest that apoptotic signals are favoured in STZ PFC with respect to the TrkB-mediated survival pathway, as reported in other neurodegenerative diseases (Ibanez and Simi, 2012), stress and depression (Ninan, 2014).

Ed-NGF treatment increases the TrkB/p75NTR ratio and TrkB phosphorylation, and reduces the levels of proBDNF thus resulting in normalisation of STZ-induced alterations in PFC. At variance with STZ, no variation in caspase-3, but a decrease of phospho-JNK level was found in PFC of STZ+NGF rats. It possible to speculate that JNK activation might correspond to other neuroprotective events triggered by ed-NGF.

The JNK pathway plays various roles, regulating neuronal survival, influences animal behaviour, and maintenance in both developing and adult brain, and thus (Yamasaki et al., 2012). Recently, JNK activation in brain has been indicated as a key event during neuro-inflammation and blood-brain barrier breakdown (Papa et al., 2004), and suppression of the JNK cascade influences inflammation in diabetic brain (Prasad et al., 2014). It is therefore likely that reduced activation of JNK following ed-NGF might be a marker of its anti-inflammatory action.

Both BDNF and NGF modulate inflammatory mediators in the brain (Prencipe et al., 2014), and NGF anti-inflammatory actions were demonstrated *in vivo* and *in vitro* (Cragnolini and Friedman, 2008). Recently, anti-inflammatory effects of ed-NGF has been shown in an animal model of brain inflammation/degeneration (Carito et al., 2015), further supporting the

ability of NGF to counteract inflammation-mediated neurodegeneration (Prencipe et al., 2014).
Since inflammation in brain is also associated with the brain plasticity and the manifestation of a depressive phenotype in both animal models and patients (Iannitelli and Tirassa, 2015), ed-NGF could, directly or throughout the regulation of BDNF, abolish the STZ-induced increase of anxiety/depression.

In summary, the present study, for the first time, demonstrates the effects of STZ and ed-NGF on BDNF signaling in the PFC and their correlation with manifestation of a depressive phenotype in adults.

9.3 Conclusions

Collectively, morphological and molecular data obtained using ed-NGF as treatment in animal models of retina and brain degeneration are consistent with a growing body of evidence demonstrating that NGF might interfere with pathological processes of neuronal cell loss. Such action might involve regulatory and modulatory effects in different cells types, including neurons and neuronal cell precursors, glial and endothelial cells.
By increasing the availability of mature NGF, ed-NGF might rebalance the Trk/p75NTR ratio to favour intracellular signals promoting survival, regrowth, neurogenesis, and plasticity. NGF might regulate angiogenesis and inflammation, either directly, or through different factors. All these events may underlie NGF involvement in the control of healthy and disease conditions.
A summary of the possible ed-NGF-targeted cell types and factors, and the intracellular pathways involved, is given in Fig. 9.1.

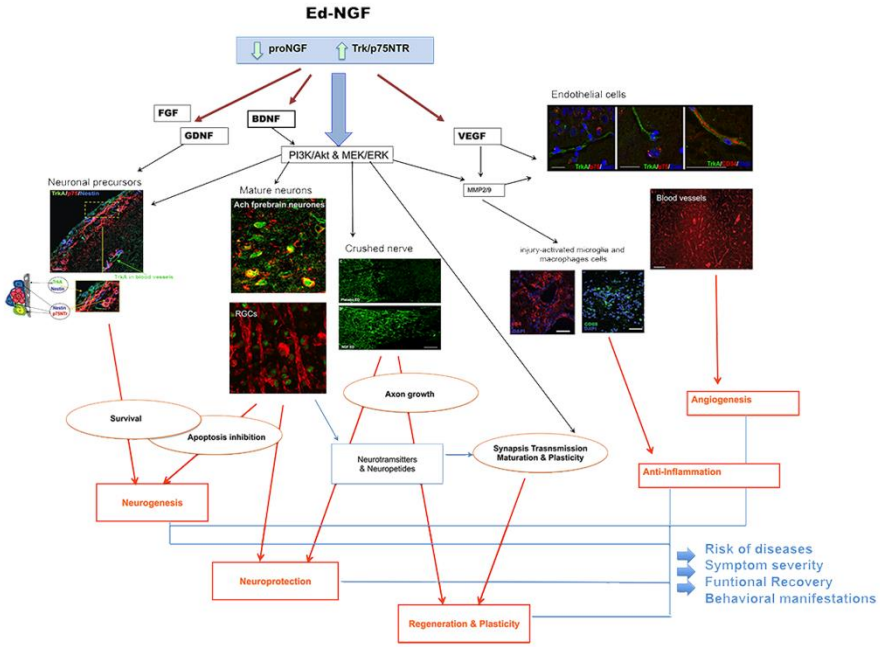

Fig. 9.1 Schematic illustration of the cell targets and mechanism of action of ed-NGF (Tirassa et al., 2017).

References

1. Aguayo AJ, Vidal-Sanz M, Villegas-Perez MP, Bray GM (1987) Growth and connectivity of axotomized retinal neurons in adult rats with optic nerves substituted by PNS grafts linking the eye and the midbrain. Ann N Y Acad Sci 495:1-9.
2. Ahmad I, Tang L, Pham H (2000) Identification of neural progenitors in the adult mammalian eye. Biochem Biophys Res Commun 270:517-521.
3. Ahmed Z, Suggate EL, Brown ER, Dent RG, Armstrong SJ, Barrett LB, Berry M, Logan A (2006) Schwann cell-derived factor-induced modulation of the NgR/p75NTR/EGFR axis disinhibits axon growth through CNS myelin in vivo and in vitro. Brain 129:1517-1533.
4. Almasieh M, Wilson AM, Morquette B, Cueva Vargas JL, Di Polo A (2012) The molecular basis of retinal ganglion cell death in glaucoma. Prog Retin Eye Res 31:152-181.
5. Almeida RD, Duarte CB (2014) p75NTR processing and signaling: functional role. In: Handbook of neurotoxicity, pp 1899-1923: Springer.
6. Aloe L, Tirassa P, Lambiase A (2008) The topical application of nerve growth factor as a pharmacological tool for human corneal and skin ulcers. Pharmacol Res 57:253-258.
7. Aston-Jones G, Chen S, Zhu Y, Oshinsky ML (2001) A neural circuit for circadian regulation of arousal. Nat Neurosci 4:732-738.
8. Bai Y, Dergham P, Nedev H, Xu J, Galan A, Rivera JC, ZhiHua S, Mehta HM, Woo SB, Sarunic MV, Neet KE, Saragovi HU (2010) Chronic and acute models of retinal neurodegeneration TrkA activity are neuroprotective whereas p75NTR activity is neurotoxic through a paracrine mechanism. J Biol Chem 285:39392-39400.
9. Balzamino BO, Esposito G, Marino R, Keller F, Micera A (2015) NGF Expression in Reelin-Deprived Retinal Cells: A Potential Neuroprotective Effect. Neuromolecular Med 17:314-325.
10. Bathina S, Das UN (2015) Brain-derived neurotrophic factor and its clinical implications. Arch Med Sci 11:1164-1178.
11. Bear MF, Connors BW, Paradiso MA (2007) Neuroscienze. Esplorando il cervello. Con CD-ROM: Elsevier srl.

12. Benowitz L, Yin Y (2008) Rewiring the injured CNS: lessons from the optic nerve. Exp Neurol 209:389-398.
13. Berson DM, Dunn FA, Takao M (2002) Phototransduction by retinal ganglion cells that set the circadian clock. Science 295:1070-1073.
14. Borsook D, Becerra L, Carlezon WA, Jr., Shaw M, Renshaw P, Elman I, Levine J (2007) Reward-aversion circuitry in analgesia and pain: implications for psychiatric disorders. Eur J Pain 11:7-20.
15. Bray GM, Villegas-Perez MP, Vidal-Sanz M, Carter DA, Aguayo AJ (1991) Neuronal and nonneuronal influences on retinal ganglion cell survival, axonal regrowth, and connectivity after axotomy. Ann N Y Acad Sci 633:214-228.
16. Butowt R, von Bartheld CS (2001) Sorting of internalized neurotrophins into an endocytic transcytosis pathway via the Golgi system: Ultrastructural analysis in retinal ganglion cells. J Neurosci 21:8915-8930.
17. Calza A, Florenzano F, Pellegrini D, Tirassa P (2011) Time-dependent activation of c-fos in limbic brain areas by ocular administration of nerve growth factor in adult rats. J Ocul Pharmacol Ther 27:209-218.
18. Carito V, Nicolo S, Fiore M, Maccarone M, Tirassa P (2015) Ocular nerve growth factor administration (oNGF) affects disease severity and inflammatory response in the brain of rats with experimental allergic encephalitis (EAE). Can J Physiol Pharmacol:1-8.
19. Carmignoto G, Maffei L, Candeo P, Canella R, Comelli C (1989) Effect of NGF on the survival of rat retinal ganglion cells following optic nerve section. J Neurosci 9:1263-1272.
20. Carmignoto G, Comelli MC, Candeo P, Cavicchioli L, Yan Q, Merighi A, Maffei L (1991) Expression of NGF receptor and NGF receptor mRNA in the developing and adult rat retina. Exp Neurol 111:302-311.
21. Castillo-Gomez E, Coviello S, Perez-Rando M, Curto Y, Carceller H, Salvador A, Nacher J (2015) Streptozotocin diabetic mice display depressive-like behavior and alterations in the structure, neurotransmission and plasticity of medial prefrontal cortex interneurons. Brain Res Bull 116:45-56.
22. Chao MV (1994) The p75 neurotrophin receptor. J Neurobiol 25:1373-1385.

23. Chao MV, Hempstead BL (1995) p75 and Trk: a two-receptor system. Trends Neurosci 18:321-326.
24. Cheung N, Mitchell P, Wong TY (2010) Diabetic retinopathy. Lancet 376:124-136.
25. Coassin M, Lambiase A, Sposato V, Micera A, Bonini S, Aloe L (2008) Retinal p75 and bax overexpression is associated with retinal ganglion cells apoptosis in a rat model of glaucoma. Graefes Arch Clin Exp Ophthalmol 246:1743-1749.
26. Colafrancesco V, Coassin M, Rossi S, Aloe L (2011) Effect of eye NGF administration on two animal models of retinal ganglion cells degeneration. Ann Ist Super Sanita 47:284-289.
27. Cosker KE, Courchesne SL, Segal RA (2008) Action in the axon: generation and transport of signaling endosomes. Curr Opin Neurobiol 18:270-275.
28. Cragnolini AB, Friedman WJ (2008) The function of p75NTR in glia. Trends Neurosci 31:99-104.
29. Cuello AC, Bruno MA, Allard S, Leon W, Iulita MF (2010) Cholinergic involvement in Alzheimer's disease. A link with NGF maturation and degradation. J Mol Neurosci 40:230-235.
30. Cuenca N, Fernandez-Sanchez L, Campello L, Maneu V, De la Villa P, Lax P, Pinilla I (2014) Cellular responses following retinal injuries and therapeutic approaches for neurodegenerative diseases. Prog Retin Eye Res 43:17-75.
31. Cui Q (2006) Actions of neurotrophic factors and their signaling pathways in neuronal survival and axonal regeneration. Mol Neurobiol 33:155-179.
32. Davies AM (1997) Neurotrophins: the yin and yang of nerve growth factor. Curr Biol 7:R38-40.
33. Dwivedi Y (2013) Involvement of brain-derived neurotrophic factor in late-life depression. Am J Geriatr Psychiatry 21:433-449.
34. Elliott AS, Weiss ML, Nunez AA (1995) Direct retinal communication with the peri-amygdaloid area. Neuroreport 6:806-808.
35. Erskine L, Herrera E (2014) Connecting the retina to the brain. ASN Neuro 6.
36. Falsini B, Iarossi G, Chiaretti A, Ruggiero A, Manni L, Galli-Resta L, Corbo G, Abed E (2016) NGF eye-drops topical administration

in patients with retinitis pigmentosa, a pilot study. J Transl Med 14:8.
37. Garcia TB, Hollborn M, Bringmann A (2017) Expression and signaling of NGF in the healthy and injured retina. Cytokine Growth Factor Rev 34:43-57.
38. Gupta N, Mansoor S, Sharma A, Sapkal A, Sheth J, Falatoonzadeh P, Kuppermann B, Kenney M (2013) Diabetic retinopathy and VEGF. Open Ophthalmol J 7:4-10.
39. Hampp G, Ripperger JA, Houben T, Schmutz I, Blex C, Perreau-Lenz S, Brunk I, Spanagel R, Ahnert-Hilger G, Meijer JH, Albrecht U (2008) Regulation of monoamine oxidase A by circadian-clock components implies clock influence on mood. Curr Biol 18:678-683.
40. Hatori M, Panda S (2010) The emerging roles of melanopsin in behavioral adaptation to light. Trends Mol Med 16:435-446.
41. Hattar S, Liao HW, Takao M, Berson DM, Yau KW (2002) Melanopsin-containing retinal ganglion cells: architecture, projections, and intrinsic photosensitivity. Science 295:1065-1070.
42. He XL, Garcia KC (2004) Structure of nerve growth factor complexed with the shared neurotrophin receptor p75. Science 304:870-875.
43. Huang EJ, Reichardt LF (2003) Trk receptors: roles in neuronal signal transduction. Annu Rev Biochem 72:609-642.
44. Hughes PM, Olejnik O, Chang-Lin JE, Wilson CG (2005) Topical and systemic drug delivery to the posterior segments. Adv Drug Deliv Rev 57:2010-2032.
45. Hut RA, Van der Zee EA (2011) The cholinergic system, circadian rhythmicity, and time memory. Behav Brain Res 221:466-480.
46. Iannitelli A, Tirassa P (2015) Pain and depression: The janus factor of human suffering. An Introduction to Pain and Its Relation to Nervous System Disorders:317.
47. Ibanez CF, Simi A (2012) p75 neurotrophin receptor signaling in nervous system injury and degeneration: paradox and opportunity. Trends Neurosci 35:431-440.
48. Johnson EM, Jr., Taniuchi M, Clark HB, Springer JE, Koh S, Tayrien MW, Loy R (1987) Demonstration of the retrograde transport of nerve growth factor receptor in the peripheral and central nervous system. J Neurosci 7:923-929.

49. Kaas JH, Balaram P (2014) Current research on the organization and function of the visual system in primates. Eye Brain 6:1-4.
50. Kahle P, Barker PA, Shooter EM, Hertel C (1994) p75 nerve growth factor receptor modulates p140trkA kinase activity, but not ligand internalization, in PC12 cells. J Neurosci Res 38:599-606.
51. Kaplan DR, Hempstead BL, Martin-Zanca D, Chao MV, Parada LF (1991) The trk proto-oncogene product: a signal transducing receptor for nerve growth factor. Science 252:554-558.
52. Katon WJ (2008) The comorbidity of diabetes mellitus and depression. Am J Med 121:S8-15.
53. Krishnan V, Nestler EJ (2011) Animal models of depression: molecular perspectives. Curr Top Behav Neurosci 7:121-147.
54. Lamba D, Karl M, Reh T (2008) Neural regeneration and cell replacement: a view from the eye. Cell Stem Cell 2:538-549.
55. Lambiase A, Aloe L (1996) Nerve growth factor delays retinal degeneration in C3H mice. Graefes Arch Clin Exp Ophthalmol 234 Suppl 1:S96-100.
56. Lambiase A, Mantelli F, Bonini S (2010) Nerve growth factor eye drops to treat glaucoma. Drug News Perspect 23:361-367.
57. Lambiase A, Tirassa P, Micera A, Aloe L, Bonini S (2005) Pharmacokinetics of conjunctivally applied nerve growth factor in the retina and optic nerve of adult rats. Invest Ophthalmol Vis Sci 46:3800-3806.
58. Lambiase A, Coassin M, Tirassa P, Mantelli F, Aloe L (2009a) Nerve growth factor eye drops improve visual acuity and electrofunctional activity in age-related macular degeneration: a case report. Ann Ist Super Sanita 45:439-442.
59. Lambiase A, Bonini S, Micera A, Rama P, Bonini S, Aloe L (1998) Expression of nerve growth factor receptors on the ocular surface in healthy subjects and during manifestation of inflammatory diseases. Invest Ophthalmol Vis Sci 39:1272-1275.
60. Lambiase A, Mantelli F, Sacchetti M, Rossi S, Aloe L, Bonini S (2011) Clinical applications of NGF in ocular diseases. Arch Ital Biol 149:283-292.
61. Lambiase A, Bonini S, Manni L, Ghinelli E, Tirassa P, Rama P, Aloe L (2002) Intraocular production and release of nerve growth factor after iridectomy. Invest Ophthalmol Vis Sci 43:2334-2340.

62. Lambiase A, Aloe L, Mantelli F, Sacchetti M, Perrella E, Bianchi P, Rocco ML, Bonini S (2012) Capsaicin-induced corneal sensory denervation and healing impairment are reversed by NGF treatment. Invest Ophthalmol Vis Sci 53:8280-8287.
63. Lambiase A, Aloe L, Centofanti M, Parisi V, Bao SN, Mantelli F, Colafrancesco V, Manni GL, Bucci MG, Bonini S, Levi-Montalcini R (2009b) Experimental and clinical evidence of neuroprotection by nerve growth factor eye drops: Implications for glaucoma. Proc Natl Acad Sci U S A 106:13469-13474.
64. Lee R, Kermani P, Teng KK, Hempstead BL (2001) Regulation of cell survival by secreted proneurotrophins. Science 294:1945-1948.
65. LeGates TA, Fernandez DC, Hattar S (2014) Light as a central modulator of circadian rhythms, sleep and affect. Nat Rev Neurosci 15:443-454.
66. Levi-Montalcini R (1987) The nerve growth factor 35 years later. Science 237:1154-1162.
67. Levi-Montalcini R, Angeletti PU (1968) Nerve growth factor. Physiol Rev 48:534-569.
68. Levi-Montalcini R, Meyer H, Hamburger V (1954) In vitro experiments on the effects of mouse sarcomas 180 and 37 on the spinal and sympathetic ganglia of the chick embryo. Cancer Res 14:49-57.
69. Longo FM, Massa SM (2013) Small-molecule modulation of neurotrophin receptors: a strategy for the treatment of neurological disease. Nat Rev Drug Discov 12:507-525.
70. Luo DG, Xue T, Yau KW (2008) How vision begins: an odyssey. Proc Natl Acad Sci U S A 105:9855-9862.
71. Maday S, Twelvetrees AE, Moughamian AJ, Holzbaur EL (2014) Axonal transport: cargo-specific mechanisms of motility and regulation. Neuron 84:292-309.
72. Matusica D, Skeldal S, Sykes AM, Palstra N, Sharma A, Coulson EJ (2013) An intracellular domain fragment of the p75 neurotrophin receptor (p75(NTR)) enhances tropomyosin receptor kinase A (TrkA) receptor function. J Biol Chem 288:11144-11154.
73. Maurice DM (2002) Drug delivery to the posterior segment from drops. Surv Ophthalmol 47 Suppl 1:S41-52.
74. Mesentier-Louro LA, De Nicolo S, Rosso P, De Vitis LA, Castoldi V, Leocani L, Mendez-Otero R, Santiago MF, Tirassa P, Rama P,

Lambiase A (2017) Time-Dependent Nerve Growth Factor Signaling Changes in the Rat Retina During Optic Nerve Crush-Induced Degeneration of Retinal Ganglion Cells. Int J Mol Sci 18.
75. Miller FD, Kaplan DR (2001) On Trk for retrograde signaling. Neuron 32:767-770.
76. Mohamed R, El-Remessy AB (2015) Imbalance of the Nerve Growth Factor and Its Precursor: Implication in Diabetic Retinopathy. J Clin Exp Ophthalmol 6.
77. Mysona BA, Shanab AY, Elshaer SL, El-Remessy AB (2014) Nerve growth factor in diabetic retinopathy: beyond neurons. Expert Rev Ophthalmol 9:99-107.
78. Newman EA (2015) Glial cell regulation of neuronal activity and blood flow in the retina by release of gliotransmitters. Philos Trans R Soc Lond B Biol Sci 370.
79. Ninan I (2014) Synaptic regulation of affective behaviors; role of BDNF. Neuropharmacology 76 Pt C:684-695.
80. Okabe K, Kobayashi S, Yamada T, Kurihara T, Tai-Nagara I, Miyamoto T, Mukouyama YS, Sato TN, Suda T, Ema M, Kubota Y (2014) Neurons limit angiogenesis by titrating VEGF in retina. Cell 159:584-596.
81. Olivares AM, Althoff K, Chen GF, Wu S, Morrisson MA, DeAngelis MM, Haider N (2017) Animal Models of Diabetic Retinopathy. Curr Diab Rep 17:93.
82. Papa S, Zazzeroni F, Pham CG, Bubici C, Franzoso G (2004) Linking JNK signaling to NF-kappaB: a key to survival. J Cell Sci 117:5197-5208.
83. Pascolini D, Mariotti SP (2012) Global estimates of visual impairment: 2010. Br J Ophthalmol 96:614-618.
84. Patel A, Cholkar K, Agrahari V, Mitra AK (2013) Ocular drug delivery systems: An overview. World J Pharmacol 2:47-64.
85. Picciotto MR, Higley MJ, Mineur YS (2012) Acetylcholine as a neuromodulator: cholinergic signaling shapes nervous system function and behavior. Neuron 76:116-129.
86. Prasad S, Sajja RK, Naik P, Cucullo L (2014) Diabetes Mellitus and Blood-Brain Barrier Dysfunction: An Overview. J Pharmacovigil 2:125.
87. Prencipe G, Minnone G, Strippoli R, De Pasquale L, Petrini S, Caiello I, Manni L, De Benedetti F, Bracci-Laudiero L (2014) Nerve

growth factor downregulates inflammatory response in human monocytes through TrkA. J Immunol 192:3345-3354.
88. Reichardt LF (2006) Neurotrophin-regulated signalling pathways. Philos Trans R Soc Lond B Biol Sci 361:1545-1564.
89. Reynolds AJ, Bartlett SE, Hendry IA (1998) Signalling events regulating the retrograde axonal transport of 125I-beta nerve growth factor in vivo. Brain Res 798:67-74.
90. Reynolds AJ, Heydon K, Bartlett SE, Hendry IA (1999) Evidence for phosphatidylinositol 4-kinase and actin involvement in the regulation of 125I-beta-nerve growth factor retrograde axonal transport. J Neurochem 73:87-95.
91. Roberti G, Mantelli F, Macchi I, Massaro-Giordano M, Centofanti M (2014) Nerve growth factor modulation of retinal ganglion cell physiology. J Cell Physiol 229:1130-1133.
92. Rosso P, Moreno S, Fracassi A, Rocco ML, Aloe L (2015) Nerve growth factor and autophagy: effect of nasal anti-NGF-antibodies administration on Ambra1 and Beclin-1 expression in rat brain. Growth Factors 33:401-409.
93. Roux PP, Barker PA (2002) Neurotrophin signaling through the p75 neurotrophin receptor. Prog Neurobiol 67:203-233.
94. Rudzinski M, Wong TP, Saragovi HU (2004) Changes in retinal expression of neurotrophins and neurotrophin receptors induced by ocular hypertension. J Neurobiol 58:341-354.
95. Sacchetti M, Lambiase A (2014) Diagnosis and management of neurotrophic keratitis. Clin Ophthalmol 8:571-579.
96. Sivilia S, Giuliani A, Fernandez M, Turba ME, Forni M, Massella A, De Sordi N, Giardino L, Calza L (2009) Intravitreal NGF administration counteracts retina degeneration after permanent carotid artery occlusion in rat. BMC Neurosci 10:52.
97. Sleipness EP, Sorg BA, Jansen HT (2007) Diurnal differences in dopamine transporter and tyrosine hydroxylase levels in rat brain: dependence on the suprachiasmatic nucleus. Brain Res 1129:34-42.
98. Sofroniew MV, Howe CL, Mobley WC (2001) Nerve growth factor signaling, neuroprotection, and neural repair. Annu Rev Neurosci 24:1217-1281.
99. Sposato V, Parisi V, Manni L, Antonucci MT, Di Fausto V, Sornelli F, Aloe L (2009) Glaucoma alters the expression of NGF and NGF

receptors in visual cortex and geniculate nucleus of rats: effect of eye NGF application. Vision Res 49:54-63.
100. Teng HK, Teng KK, Lee R, Wright S, Tevar S, Almeida RD, Kermani P, Torkin R, Chen ZY, Lee FS, Kraemer RT, Nykjaer A, Hempstead BL (2005) ProBDNF induces neuronal apoptosis via activation of a receptor complex of p75NTR and sortilin. J Neurosci 25:5455-5463.
101. Teng KK, Felice S, Kim T, Hempstead BL (2010) Understanding proneurotrophin actions: Recent advances and challenges. Dev Neurobiol 70:350-359.
102. Thrimawithana TR, Young S, Bunt CR, Green C, Alany RG (2011) Drug delivery to the posterior segment of the eye. Drug Discov Today 16:270-277.
103. Tirassa P (2011) The nerve growth factor administrated as eye drops activates mature and precursor cells in subventricular zone of adult rats. Arch Ital Biol 149:205-213.
104. Tirassa P, Maccarone M, Florenzano F, Cartolano S, De Nicolo S (2013) Vascular and neuronal protection induced by the ocular administration of nerve growth factor in diabetic-induced rat encephalopathy. CNS Neurosci Ther 19:307-318.
105. Tirassa P, Maccarone M, Carito V, De Nicolo S, Fiore M (2015) Ocular nerve growth factor administration counteracts the impairment of neural precursor cell viability and differentiation in the brain subventricular area of rats with streptozotocin-induced diabetes. Eur J Neurosci 41:1207-1218.
106. Tirassa P, Iannitelli A, Sornelli F, Cirulli F, Mazza M, Calza A, Alleva E, Branchi I, Aloe L, Bersani G, Pacitti F (2012) Daily serum and salivary BDNF levels correlate with morning-evening personality type in women and are affected by light therapy. Riv Psichiatr 47:527-534.
107. Tropepe V, Coles BL, Chiasson BJ, Horsford DJ, Elia AJ, McInnes RR, van der Kooy D (2000) Retinal stem cells in the adult mammalian eye. Science 287:2032-2036.
108. van Dijk HW, Verbraak FD, Stehouwer M, Kok PH, Garvin MK, Sonka M, DeVries JH, Schlingemann RO, Abramoff MD (2010) Association of visual function and ganglion cell layer thickness in patients with diabetes mellitus type 1 and no or minimal diabetic retinopathy. Vision Res 51:224-228.

109. Vandewalle G, Maquet P, Dijk DJ (2009) Light as a modulator of cognitive brain function. Trends Cogn Sci 13:429-438.
110. Vandewalle G, Schmidt C, Albouy G, Sterpenich V, Darsaud A, Rauchs G, Berken PY, Balteau E, Degueldre C, Luxen A, Maquet P, Dijk DJ (2007) Brain responses to violet, blue, and green monochromatic light exposures in humans: prominent role of blue light and the brainstem. PLoS One 2:e1247.
111. von Bartheld CS (1998) Neurotrophins in the developing and regenerating visual system. Histol Histopathol 13:437-459.
112. Von Bartheld CS, Williams R, Lefcort F, Clary DO, Reichardt LF, Bothwell M (1996) Retrograde transport of neurotrophins from the eye to the brain in chick embryos: roles of the p75NTR and trkB receptors. Journal of Neuroscience 16:2995-3008.
113. Wahle P, Di Cristo G, Schwerdtfeger G, Engelhardt M, Berardi N, Maffei L (2003) Differential effects of cortical neurotrophic factors on development of lateral geniculate nucleus and superior colliculus neurons: anterograde and retrograde actions. Development 130:611-622.
114. Waiczies H, Millward JM, Lepore S, Infante-Duarte C, Pohlmann A, Niendorf T, Waiczies S (2012) Identification of cellular infiltrates during early stages of brain inflammation with magnetic resonance microscopy. PLoS One 7:e32796.
115. Waite D, Wang Y, Jones D, Stitt A, Raj Singh TR (2017) Posterior drug delivery via periocular route: challenges and opportunities. Ther Deliv 8:685-699.
116. Wang KC, Kim JA, Sivasankaran R, Segal R, He Z (2002) P75 interacts with the Nogo receptor as a co-receptor for Nogo, MAG and OMgp. Nature 420:74-78.
117. Wiesmann C, de Vos AM (2001) Nerve growth factor: structure and function. Cell Mol Life Sci 58:748-759.
118. Yantis S (2014) Sensation and perception: Palgrave Macmillan.
119. Yiu G, He Z (2006) Glial inhibition of CNS axon regeneration. Nat Rev Neurosci 7:617-627.
120. Zhang Y, Moheban DB, Conway BR, Bhattacharyya A, Segal RA (2000) Cell surface Trk receptors mediate NGF-induced survival while internalized receptors regulate NGF-induced differentiation. J Neurosci 20:5671-5678.

Supplementary Chapter

MATERIALS AND METHODS

S.1 Study on optic nerve crush models

S.1.1 Animals

Pathogen-free adult Long Evans rats (male, 300-350 g), purchased from Charles River (Charles River Laboratories Italia s.r.l), were used in accordance with the ARVO Statement for the Use of Animals in Ophthalmic and Vision Research, and after the Animal Care and Use Committee of the San Raffaele Scientific Institute approval. All procedures were performed under anesthesia with ketamine and xylazine and every effort was made to minimize suffering.

The rats were divided in two groups: Control naïve rats (CTR), which were used to measure basal levels of neuronal cell marker expression and intracellular pathway activation, and rats submitted to unilateral optic nerve crush (Crush group) following the procedure described below. Rats in the Crush group were sacrificed at different time points, such as 1,3,7 and 14 after days after crush (dac) to evaluate the time-dependent changes occurring in the retina.

The effects of ONC on the functional and structural integrity of the retina were evaluated by in vivo analysis and by morphological and biochemical techniques, as described below.

S.1.2 Optic nerve Crush (ONC)

ONC was performed as described previously (Mesentier-Louro et al., 2012). Briefly, animals were anesthetized by intraperitoneal injection of ketamine (70 mg/Kg) and xylazine (10 mg/Kg) and topical application of oxybuprocaine 0.4% eye drops. Ophthalmic eye ointment was applied to avoid dehydration and damage of the ocular surface. Under a stereoscopic microscope, the left optic nerve was accessed after an incision to the skin covering the orbital bone, and the dura mater surrounding the nerve was cut longitudinally. Nerve crush was performed by compression with tweezers (Dumont #5, 45° angle, 0.05 x 0.01 mm tips, World Precision Instruments, Sarasota, FL, USA) for 15 s, at 1 mm behind the eye, with care to avoid damage to the blood vessels. Before and after the procedure, the back of the eye was observed through the microscope to assess integrity of the retinal blood flow. Animals with damage to the lens or retinal blood vessels were excluded. After the procedure, the incision in the skin was sutured and topical antibiotic (Levofloxacin 5 mg/ml) was applied. Right eyes were left untouched (intact nerve) and served as internal control, indicated as contralateral eye (CoEye). Animals were placed in a recovery cage with a heat pad and given a subcutaneous injection of Carprofen (5 mg/Kg) for postoperative analgesia. From a total of 90 only 6 rats did not survive or well recover well from surgery and therefore were not included in the study.

S.1.3 NGF treatment and Experimental design

A first set of experiments was performed to evaluate the effects of intravitreal (ivt) and topical eye drops (ed) application of NGF on RGC survival and axon growth in the ONC model. Thirty rats received ivt- or ed- administration with rhNGF or vehicle in the left eye with crushed nerve (ONC eye). The first group of rats received a first ivt injection with 1-1.5µg/eye of rhNGF (ivt-

rhNGF), or vehicle immediately after crush, and a second injection at 72 hrs post-crush.

A second group of ONC rats received a droplet of 10 μL of rhNGF or vehicle (ed-vehicle) on the ocular surface immediately after crush and then twice a day from day 1 after crash for 7 or 14 days. Based on previous observations on the efficacy of ed-NGF (Lambiase et al., 2009), two concentrations of rhNGF were used for topical administration: 180 μg/ml (ed-rhNGF 180) and 540 μg/ml (ed-rhNGF 540).

A group of naïve rats was used as further control (CTR) to evaluate the basal condition and disclose possible effects of ONC and/or the ocular treatment on CoEye.

Retina flat-mount preparations and nerve sections were used for RGC counts and axon growth quantification following immunofluorescence staining (Fig.S1).

A second set of experiment was performed to further characterize the effects of ed-treatment. A total of 54 ONC rats were divided in three experimental groups, such as ed-vehicle, ed-rhNGF180, and ed-rhNGF 540. Retina flat-mount preparations and nerve sections from rats (n=6 per group) at 14 dac were processed for immunofluorescence and used for RGC counts and axon growth quantification (Fig. S2).

Six rats for each treatment group were sacrificed at 7 and 14 dac by decapitation to collect the fresh retinas and nerves to be processed for protein extraction and WB as described below. Three healthy and untreated rats were used as further control in the biochemical assays.

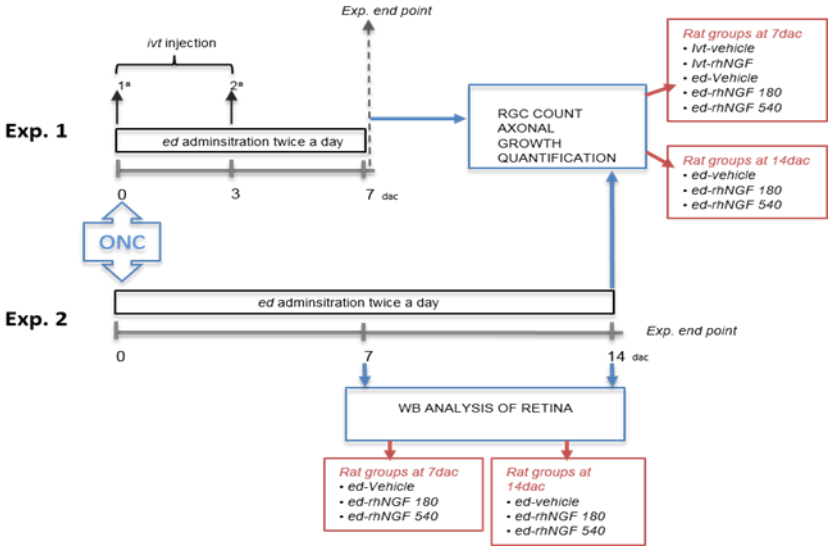

Fig. S1 Scheme of the study design.

S.1.4 Molecular Analysis

S.1.4.1 Retina dissection and Protein Extraction

Six CTR rats and 24 Crush rats (6 per time point) were sacrificed by cervical dislocation. The eyes were rapidly excised and the left (Crush) and right (CoEye) retinas were dissected on ice and stored in clean sterile tubes at -80°C until use. For protein extraction, retinal samples were homogenized by ultrasonication in lysis buffer (20 mM Tris–acetate, pH 7.5; 150 mM NaCl; 1 mM EDTA; 1 mM EGTA, 2.5 mM sodium-pyrophosphate, 1 mM orthovanadate, 1 mM (R)-glycerolphosphate, 100 mM NaF, 1 mM phenylmethylsulfonyl fluoride and 1 mg/mL leupeptin) and then kept one hour in the cold room on a rotating shaker to allow complete tissue/cell dissociation. After centrifugation at 10000 rpm for 30 min at 4°C the supernatants were used for total protein concentration measured by the Biorad assay, ELISA, PathScan assay and WB analysis as described below.

S.1.4.2 Western Blot analysis

Sample (20-50 µg total protein) were dissolved in loading buffer (0.1 mol/L Tris–HCl buffer, pH 6.8, containing 0.2 mol/L DTT (Ditiotreitolo), 4% SDS, 20% glycerol, and 0.1% bromophenol blue), separated by SDS-PAGE, and electrophoretically transferred to polyvinylidene fluoride (PVDF) or nitrocellulose membranes. The membranes were incubated for 1 h at room temperature (RT) with 5% non-fat dried milk dissolved in TBS-T (10 mmol/L Tris, pH 7.5, 100 mmol/L NaCl and 0.1% Tween-20), washed three times for 10 min each in TBS-T, and then incubated overnight at 4°C with primary antibody (Table 1). Horseradish peroxidase-conjugated anti-rabbit IgG (Cell Signaling Technology, Danvers, MA, USA) was used as a secondary antibody. The blots were developed with ECL Chemiluminescent HRP

Substrate (Sigma, Darmstadt, Germany) as the chromophore. The public-domain ImageJ software was used for densitometry. The integrated density of glyceraldehyde 3-phosphate dehydrogenase (anti-rabbit GAPDH-HRP conjugate antibody; Cell Signaling Technology) served as the normalizing factor (housekeeping protein). Six retinas were used for each group (CTR, Crush or CoEye), at each time point. Values are expressed as arbitrary OD units and presented as means±SEM or means±s.d.

Antibody	*Company*	*Host*	*Dilution*
GFAP	Abcam, Cambridge, UK	Rabbit	1:20000
proNGF	Alomone, Jerusalem, Israel	Rabbit	1:500
TrkA	Cell signaling Technology, USA	Rabbit	1:1000
pTrkA	Cell signaling Technology, USA	Rabbit	1:1000
p75	Cell signaling Technology, USA	Rabbit	1:1000
pERK	Cell signaling Technology, USA	Mouse	1:1000
ERK	Cell signaling Technology, USA	Rabbit	1:1000
pAKT	Cell signaling Technology, USA	Rabbit	1:1000
AKT	Cell signaling Technology, USA	Mouse	1:1000

Table 1. Primary antibodies used for Western Blot analysis.

S.1.4.3 Neurotrophin concentrations

NGF concentration in the retina was measured by ELISA assay using the rat β-NGF Duoset Elisa (R&D Systems, Inc., Minneapolis, MN, USA), following the manufacturer's instructions. The assay is specific for rat b-NGF with approximately 0.1% and 50% cross-reactivity with human and mouse

recombinant b-NGF respectively, and has no cross-reactivity with other human or rat growth factors. The colorimetric reaction product was measured at 450 nm. Results are expressed as pg/mg protein (mean±SEM).

S.1.4.4 Activated Intracellular signal pathways

The PathScan Intracellular Signaling array kit (Cell Signalling Technology) was used, according to the manufacturer's instructions, to detect the nerve crush-induced phosphorylation or cleavage of signaling molecules in the retina. The kit allows the simultaneous detection of 18 signaling molecules when phosphorylated, including ERK1/2 (Thr102/Tyr204), Stat1 (Tyr701), Stat3 (Tyr705), AKT (Thr308), AKT (Ser473), AMPKa (Thr172), S6 Ribosomal Protein (Ser235/236), mTOR (Ser2448), HSP27 (Ser78), BAD (Ser112), p70S6K (Thr389), PRAS40 (Thr246), p53 (Ser15), p38 (Thr180/Tyr182), SAPK/JNK (Thr183/Tyr185) and GSK-3beta (Ser9); or cleaved, including PARP (Asp214) and caspase-3 (Asp175), by which it is possible to investigate the activation of proteins involved in cell cycling, growth, and survival. Protein samples were diluted in array diluent buffer to 1 mg/mL. Glass slides with antibody spotted nitrocellulose-pads were connected with a multi-well gasket for blocking each pad with blocking buffer for 15 min, followed by 16 h incubation at 4°C with diluted samples/well. After four washing steps, the pads were incubated with detection antibody cocktail for 1 h at room temperature (R.T). LumiGLO Reagent was used to reveal the bound detection antibody by chemiluminescence. The images were captured with the UVItec gel documentation system (UVItec Limited, Cambridge, UK) and spot intensities were quantified using Nikon NIS-Elements AR 2.30 software (Nikon Instruments Europe BV, Amsterdam, The Netherlands). A fixed threshold over the background, and feature restriction functions were applied to define

the measurable spot area and intensity. Measurements were standardized between the experimental groups using the same calibration system and threshold. Data are expressed as mean optical density (arbitrary units) and presented as mean±SEM.

S.1.5 Morphological Analysis

For histological evaluation of the optic nerve and retina, rats at 7 and 14 dac were anesthetized with an overdose of ketamine and xylazine before killing by transcardial perfusion with ice-cold saline, followed by 4% paraformaldehyde (pH 7.4). The eyes and optic nerves were cleaned of connective tissue and post-fixed in 4% paraformaldehyde for 2 h at 8–10°C.

S.1.5.1 Immunofluorescence (IF)

The retinas were dissected and processed for whole-mount preparations. Retina whole-mount samples were processed for immunostaining detection of RGCs. Primary antibodies (Table 2) were diluted in PBS with 0.2% Triton X-100 (PBS-T) and 5% normal donkey serum (Sigma-Aldrich, St. Louis, MO, USA) and incubated overnight at 4°C. Retinas were washed three times in PBS and incubated with the secondary antibodies Alexa 488 donkey anti-goat IgG Alexa Fluor 546 donkey anti-mouse IgG (1:1000, Life Technologies, Camarillo, CA, USA) for 2 h at room temperature. The retinas were washed three times in PBS, flat-mounted, and covered with Vectashield mounting medium (Vector Laboratories, Inc., Burlingame, CA, USA). All steps were performed under gentle shaking.
The eyes and optic-nerve segments used for GFAP, p75NTR, Tuj1 and Gap-43 were transferred to PBS with increasing sucrose concentrations up to 30%. The tissue was cut longitudinally on a cryostat (Leica Microsystems,

Nussloch GmbH, Nussloch, Germany) at 14–20 µm thickness. Tissue sections were rinsed with 0.1% PBS-T and incubated with 5% normal donkey serum for 30 min at R.T to block non-specific binding. Tissue sections were incubated with primary antibody (Table 2) overnight at 4°C, washed in PBS, and then incubated with secondary antibodies: donkey anti-goat Cy3 conjugate (1:1000, Jackson Immunoresearch Laboratories, West Grove, USA), Alexa Fluor 488 donkey anti-rabbit IgG and/or Alexa Fluor 546 donkey anti-mouse IgG (1:1000, Life Technologies) for 2 h at R.T. Sections were then washed three times in PBS, mounted with Vectashield and nuclei stained with DAPI (Vector Laboratories). All immune-reacted sections were extensively analyzed and representative images were captured with a confocal microscope (TCS SP5; Leica Microsystems) and composed in Adobe Photoshop CS5 format.

Antibody	*Company*	*Host*	*Dilution*
GFAP	Abcam, Cambridge,UK	Rabbit	1:400
Tuj1	Covance, Berkeley, USA	Mouse	1:250
Brn3a	Santa Cruz Biotechnology, USA	Goat	1:250
p75NTR	Santa Cruz Biotechnology, USA	Mouse	1:100
GAP43	Santa Cruz Biotechnology, USA	Rabbit	1:50
Nogo-A	Santa Cruz Biotechnology, USA	Rabbit	1:100
p75NTR	Clone 192 (gift from E.M. Johnson	Mouse	1:50

Table 2. Primary antibodies used for immunofluorescence analysis.

S.1.5.2 RGC and axon outgrowth quantification

A total of 32 flat-mounted retinas (n = 16 for CoEye; n = 8 for Crush 7 dac; n = 8 for Crush 14 dac) were imaged by a blinded observer with the aid of a fluorescence microscope (Leica CTR5500; Leica Microsystems), with the focus positioned on the GCL. Images were randomly acquired at approximately 1.0 mm and (central retina) and 3.5 mm (peripheral retina) from the optic disc, in all quadrants of the retina. Twenty images of 0.064 mm^2 (40× magnification) were taken for Tuj1 staining, and 10 images of 0.366 mm^2 (20×magnification) were taken for Brn3a. The mean number of cells was divided by the area and normalized to the CoEye group. Data are expressed as mean±SEM. Representative images of the retinas were acquired with a confocal microscope (TCS SP5; Leica Microsystems).

For axonal growth quantification, the optic nerve sections were immunostained for Gap-43 and analyzed with a epifluorescence microscope (Leica CTR5500; Leica Microsystems). The center of the field of a 40× magnification objective lens was positioned at 0.25, 0.50, 0.75, 1.00, 1.50 and 2.00 mm from the proximal border of the crush site (Fig. S2). The values obtained were normalized by the formula described by Leon and colleagues (Leon et al., 2000) and expressed as the total number of axons per nerve at each distance from the lesion site.

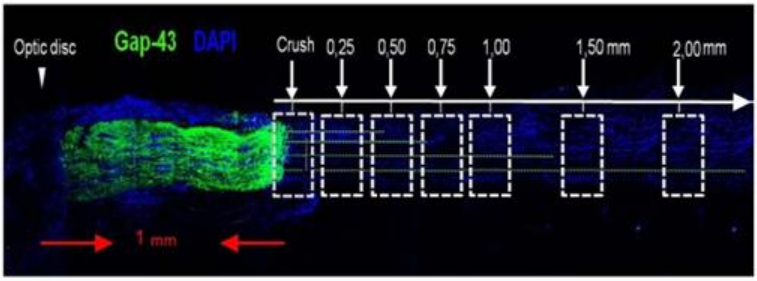

Fig. S2 Nerve section shows the field at distance points (from 0.25 to 2.00 mm) form crush site to which the GAP43 stained axons were quantified.

S.1.6 Statistical Analysis

Biochemical data were subjected to one-way analysis of variance (ANOVA) considering the CTR, CoEye and Crush groups at the indicated time points as variables. Multicomparison analysis was performed by Tukey–Kramer post hoc test. The Tuj1 and Brn3a cell counts were compared among CoEye, at 7 and 14 dac, using a one-way ANOVA with Tukey's multiple comparisons test. Gap-43 counts were compared between CoEye and Crush groups using a Student t-test at each distance analyzed, using GraphPad Prism software.

For the second part of the study axon growth measures were compared by Two-way ANOVA using the distance from crush site and treatment as variables. Biochemical data were compared with two-way ANOVA using the time, ONC and rhNGF administration ad variables. Multicomparison analysis was evaluated by Tukey–Kramer post hoc test. $p<0.05$ was considered statistically significant.

S.2 Study on STZ-induced diabetes models

S.2.1 Animals

A total of 30 Sprague Dawley adult male rats (body weight 200–250 g) were used in this study. For the housing, care, and experimental procedures, the guidelines indicated and approved by intramural Committee and Institutional Guidelines of the Italian National Research Council in conformity with National and International laws (EEC Council Directive 86/609, OJ L 358, 1, 12 December 1987) were followed. The ocular procedures were in accordance with the ARVO Statement for the Use of Animals in Ophthalmic and Vision Research, and all efforts were taken to limit the number and minimize suffering of rats.

S.2.2 Diabetes induction, experimental design and ed-NGF treatment

Diabetes was induced by an intraperitoneal injection of STZ (60 mg/kg; SigmaAldrich, St. Louis, MO, USA). Control (CTR) rats received an injection with physiological solution. Rats were allowed to drink a 10% dextrose solution overnight. The glucose level in blood was evaluated at day 0 (before intraperitoneal injection of STZ or vehicle) and after STZ injection by glucometer (Contour XT, Bayer, Germany). Rats with blood glucose levels above 250 mg/dL were diagnosed as diabetic and included in the experiment to evaluate the effects of diabetes and/or ocular NGF treatment. NGF was isolated from male mouse submaxillary salivary glands and purified by a protocol based on the method described by Bocchini and Angeletti (Bocchini and Angeletti, 1969). Purified NGF dissolved in a physiological solution (0.9% sodium chloride) at a concentration of 200 µg/mL was used during treatment.

Rats were divided into four experimental groups: healthy control groups named CTR and CTR + NGF received ocular treatment with saline and two drops (10 μL each) of 200 μg/mL NGF to both eyes, respectively; the diabetic rat group (STZ) received two drops of physiological solution per eye and the STZ + NGF group, received ed-NGF.
Ocular treatment started 6 weeks after diabetes induction and was repeated twice a day for 2 weeks. All rats were sacrificed *previa* anesthesia at 8 weeks days post induction (dpi) by decapitation. During the whole of experimental period, the rats were maintained on a 12-h light–dark cycle and provided with food and water ad libitum.

S.2.3 Diabetes Effects on Body Weight and Depressive Phenotypes

Body weight (BW) was measured weekly from day 0 and at the end of the experiment (8 weeks dpi). As reported, diabetic rats at eighth weeks after STZ induction show a depressive phenotype (Chen et al., 2014) evaluated by forced swimming test (FST), which is one widely used assay to assess antidepressant efficacy in preclinical studies (Krishnan and Nestler, 2011). FST was performed by introducing the rats into a glass cylinder with a height of 60 cm, diameter of 30 cm, water depth of 50 cm (to ensure that the adult rats were unable reach the bottom with their tails, to keep their noses above the water), and temperature of 25°C. Immobility time was considered as rats floating passively, making small movements to keep their heads above the water level (El Khoury et al., 2006; Marais et al., 2009). The development of depressive/anxiety behavior was measured by the latency for the first floating episode and immobility time (minutes). A 9-min swimming test session was carried out during the light phase of the light/dark cycle. Animals were tested under indirect dim light. At the end of each session, animals were towel-dried

and then transferred into a heated chamber (37 ± 1°C) for a 15-min warm-up period.

S.2.4 Molecular Analysis

S.2.4.1 Brain and retina dissection and Protein Extraction

Six rats per group were deeply anesthetized with an overdose of ketamine and xylazine and sacrificed by decapitation. The retina and prefrontal cortex was quickly dissected on ice and stored in clean and sterile tubes at -80°C until use. To extract proteins, the tissue samples were homogenized by ultrasonication in RIPA buffer (50 mM Tris–HCl, pH 7.4; 150 mM NaCl; 5 mM EDTA; 1% Triton X-100; 0.1% SDS; 0.5% sodium deoxycholate; 1 mM PMSF (phenylmethylsulfonyl fluoride); 1 mg/mL leupeptin), kept at 4°C on a rotary shaker for 2 h to allow for complete tissue disaggregation and cell lysis. Homogenates were centrifuged at 10,000 rpm for 30 min at 4°C. The supernatants were used for total protein concentration measured by the Bio-Rad assay, and ELISA and Western blot analysis, as described below.

S.2.4.2 Western Blot

Sample (20 or 40 µg) of total proteins were dissolved in loading buffer (0.1 M Tris–HCl buffer, pH 6.8, containing 0.2 M dithiothreitol, DTT, 4% sodium dodecyl phosphate, SDS, 20% glycerol and 0.1% bromophenol blue), separated by 8-12% SDS-PAGE, and electrophoretically transferred to nitrocellulose or polyvinylidene difluoride (PVDF) membranes.
The membranes were incubated for 1 h at RT with blocking buffer consisting of 5% nonfat dry milk in TBS-T and washed three times for 10 min each at R.T in TBS-T followed by incubation overnight at 4°C with primary

antibodies (Table 3). These steps were followed by incubation for 1 h with 1:10000 or 1:2000 goat anti-rabbit immunoglobulin (Ig) G coupled or anti-mouse IgG (Cell Signaling Technology). Immunoblot analyses were performed using a chemiluminescence detection kit (ECL) as the chromophore (Millipore, MA, USA). Relative levels of immunoreactivity were determined using densitometry and ImageJ software (National Institutes of Health, Bethesda, MD, USA) for Windows 10. Each reported value was derived from the ratio between arbitrary units obtained by the protein band and the respective glyceraldehyde-3-phosphate dehydrogenase (GAPDH) or actin (chosen as housekeeping proteins). Values are expressed as arbitrary OD units, and the data are presented as means±s.d.

Antibody	*Company*	*Host*	*Dilution*
TrkB	Santa Cruz Biotechnology, USA	Rabbit	1:1000
proBDNF	Millipore corporation, USA	Rabbit	1:1000
p75NTR	Santa Cruz Biotechnology, USA	Rabbit	1:1000
AKT	Cell Signaling Technology, USA	Rabbit	1:1000
p-AKT (Ser473)	Santa Cruz Biotechnology, USA	Rabbit	1:1000
SAPK/JNK	Cell Signaling Technology, USA	Rabbit	1:100
p-SAPK/JNK	Cell Signaling Technology,USA	Rabbit	1:1000
TrkA	Santa Cruz Biotechnology, USA	Rabbit	1:1000
p75NTR	Santa Cruz Biotechnology, USA	Mouse	1:1000
ProNGF	Alomone, Jerusalem, Israel	Rabbit	1:500
VEGF	Santa Cruz Biotechnology, USA	Mouse	1:1000
VGFR2-Flk-1 (D-8)	Santa Cruz Biotechnology, USA	Mouse	1:1000

Table 3. Primary antibodies used for Western Blot analysis.

S.2.4.3 Immunoenzymatic Activity (ELISA)

The brain concentration of BDNF was measured using an ELISA kit (BDNF EmaxTM ImmunoAssay System G7611, Promega, Madison, WI, USA) in according with the manufacturer's instructions. The colorimetric reaction product was measured at 450 nm using a microplate reader (Thermo Scientific Multiskan EX, Waltham, MA, USA). Each test was performed in duplicate, and the data expressed as pg/mg of protein and presented as mean±s.d.

Phospho-TrkB brain levels were measured using PathScan Phospho-TrkB (Tyr516) Sandwich ELISA Kit (#7111C, Cell Signaling Technology, Inc) following the protocol supplied by the manufacturer. The colorimetric reaction product was measured at 450 nm using a microplate reader (Thermo Scientific Multiskan EX). Values are expressed as arbitrary OD units, and the data are presented as means±s.d.

S.2.5 Statistical Analysis

Molecular experiments were evaluated using GraphPad Prism 5 software, and statistical analysis was conducted using one-way ANOVA. Differences between groups were determined by the Tukey–Kramer multicomparison post hoc test. Means from independent experiments were expressed as means±s.d. For all statistical analysis, values $p<0.05$ or less were considered statistically significant.

References

Bocchini V, Angeletti PU (1969) The nerve growth factor: purification as a 30,000-molecular-weight protein. Proc Natl Acad Sci U S A 64:787-794.

Chen C, Wang Y, Zhang J, Ma L, Gu J, Ho G (2014) Contribution of neural cell death to depressive phenotypes of streptozotocin-induced diabetic mice. Dis Model Mech 7:723-730.

El Khoury A, Gruber SH, Mork A, Mathe AA (2006) Adult life behavioral consequences of early maternal separation are alleviated by escitalopram treatment in a rat model of depression. Prog Neuropsychopharmacol Biol Psychiatry 30:535-540.

Krishnan V, Nestler EJ (2011) Animal models of depression: molecular perspectives. Curr Top Behav Neurosci 7:121-147.

Lambiase A, Coassin M, Tirassa P, Mantelli F, Aloe L (2009) Nerve growth factor eye drops improve visual acuity and electrofunctional activity in age-related macular degeneration: a case report. Ann Ist Super Sanita 45:439-442.

Leon S, Yin Y, Nguyen J, Irwin N, Benowitz LI (2000) Lens injury stimulates axon regeneration in the mature rat optic nerve. J Neurosci 20:4615-4626.

Marais L, Stein DJ, Daniels WM (2009) Exercise increases BDNF levels in the striatum and decreases depressive-like behavior in chronically stressed rats. Metab Brain Dis 24:587-597.

Mesentier-Louro LA, Coronel J, Zaverucha-do-Valle C, Mencalha A, Paredes BD, Abdelhay E, Mendez-Otero R, Santiago MF (2012) Cell therapy modulates expression of Tax1-binding protein 1 and synaptotagmin IV in a model of optic nerve lesion. Invest Ophthalmol Vis Sci 53:4720-4729.